IRREGULARITIES AND MODULATED DISLOCATION PATTERNS IN PLASTICALLY DEFORMED METALS: THE ECKHAUS INSTABILITY

S.N. Rashkeev[1], M.V. Glazov[2] and O. Richmond[2]

[1]*Physics Department, Case Western Reserve University, Cleveland, OH 44106-7079, USA*
[2]*Alcoa Technical Center, 100 Technical Drive, Alcoa Center, PA 15069-0001, USA*

(Submitted October 12, 1998)

ABSTRACT

Phase modulations of periodic dislocation patterns, observed in transmission electron microscopy(TEM) studies of some single crystalline metals, are analyzed using the methods of nonlinear dynamics. The Ginzburg-Landau (GL) equation for the soft mode instability in the weakly nonlinear regime is derived for the Walgraef-Aifantis (WA) model for a coupled system of two populations of dislocations. The bulk of results is obtained using the GL equation rather than the WA model itself. We demonstrate that phase modulations of dislocation patterns can be described using the concept of the Eckhaus instability which describes one of the most fundamental "generic" mechanisms of wavelength-changing and which was successfully used before for the analysis of nonlinear systems of different physico-chemical nature. The timescale of wavelength-changing processes in dislocation systems can be very large when the system is close to the Eckhaus stability limit, i.e., the metastable phase modulations of dislocation pattern can survive nearly unchanged for a long time. The results of numerical simulations for realistic values of the parameters show that the Eckhaus instability could be the underlying physical reason for modulated ladder structures of PSBs in cyclically deformed metallic alloys.

I. INTRODUCTION

The collective behavior of dislocation ensembles plays a crucial role in many practically important phenomena, such as work hardening, dislocation patterning in plastically deformed metals, and the Portevin-Le Chatelier effect in monotonically or cyclically loaded metals. In particular, the formation of Persistent Slip Bands (PSBs) is thought of as a material instability at the mesoscale resulting in the formation of regular arrays of dislocation walls /1-9/. The wavelength of the PSBs (they are called persistent because, being removed by surface polishing, they reappear at the same locations if the cyclic stress is continued) and the average distance between two adjacent walls are determined by the intrinsic length scales introduced via generalized dislocation mobilities coefficients.

In spite of the fact that many properties of an individual dislocation were successfully studied theoretically /10,11/ as well as in atomistic simulations /12-15/, it is still not an easy task to make a connection between an atomistic scale and a mesoscopic level on which dislocation patterning develops. A successful attempt at establishing such a connection was made recently by Bulatov *et al.* /16/ who performed both atomistic and mesoscopic (by using the Peach-Koehler equation) simulations of dislocation junctions (Lomer-Cottrell locks) in a Lennard-Jones system. Nevertheless, such "success stories" are still relatively rare, and more typically mesoscopic simulations are performed in order to probe collective properties of dislocation patterning /17-20/.

Dislocation patterning in deformed metals is intimately connected with thermodynamically irreversible plastic phenomena /21/. This irreversibility makes it impossible to obtain these structures by minimizing some appropriate potential functions, i.e., one cannot simply transfer the principles of equilibrium thermodynamics to plastic instabilities /17,22/.

An alternative approach is based on a continuum description, i.e., on the study of nonlinear systems of governing equations for dislocation densities. This "self-organizational" approach considers the formation of dislocation structures as a bifurcation phenomenon leading to solutions which do not belong to the thermodynamic branch /1,2,23-25/. At the present moment there is no general way to derive these equations starting from individual dislocations and their interactions. Usually the analysis of these equations is limited to studying their linear stability, which describes only primary bifurcations corresponding, e.g., to spatially homogeneous oscillations in time (Hopf instability), or to the formation of steady-state spatial waves of dislocation densities (Turing instability). It is also important to mention the recent interesting attempts to apply the methods of stochastic dynamics to dislocation ensembles in order to describe the formations of PSBs and matrix structures /26-28/.

In many cases linear stability analysis is not sufficient to describe how an emerging dislocation pattern will react to spatio-temporal perturbations on different length and time scales. This means that one has to consider some nonlinear instabilities too. This fact has been understood for the first time in a series of papers of Aifantis and coworkers (see, e.g., Refs. /7,29,30/ and references therein). They proposed to consider the slow mode dynamics in a weakly nonlinear regime. In this case the slow or unstable modes should play a role of an "order parameter", and their dynamics is described by the time-dependent amplitude GL equation. The typical examples of nonlinear instabilities include the Benjamin-Fair instability which can cause the growth of the phase fluctuations in time and phase turbulence /31/, and the Eckhaus instability which generates phase modulations of periodic spatial patterns with a subsequent change of the pattern wavenumber /32/.

In this work we present the results of our study of the Eckhaus instability in dislocation systems which can generate structure modulations in dislocation patterns. Such modulations and irregularities have been observed many times before in the TEM studies (the TEM image exhibits the dislocation-rich and dislocation-poor regions of the sample). Figure 1 shows an experimental TEM image from Ref. /33/. It can be clearly seen that the ladder structure of PSBs in a copper single crystal is indeed modulated, and the PSB wavelength increases and decreases in a systematic way. Later, similar results

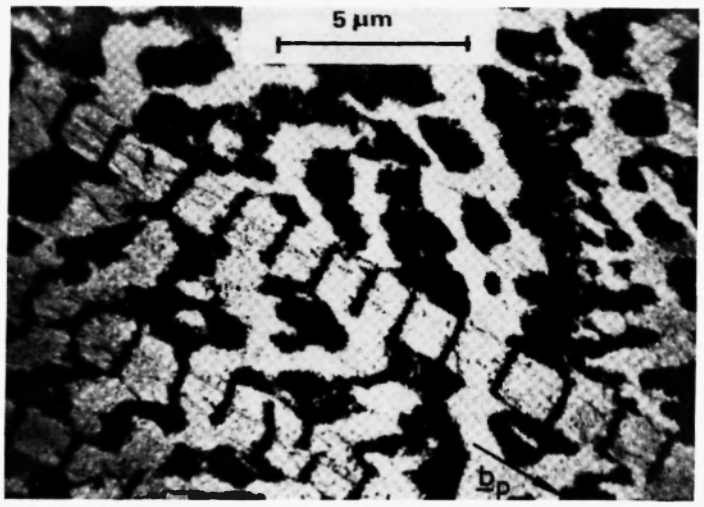

Fig. 1: The ladder structure of PSBs in a copper single crystal cycled at a strain amplitude in the plateau (the $[1\bar{2}1]-$slice is shown, the crystal is pinned in the loaded state by neutron irradiation, after Laird *et al.* /33/).

were observed in numerical simulations of Glazov and Laird /34/ within the framework of the one-dimensional "reaction + diffusion" approach and the finite-size analog of the WA-model (Figure 2). Very impressive results highlighting the dynamical evolution of dislocation structures have been recently obtained by Holzwarth and Essmann /35/ who considered the transformation of irregular, amoeba-shaped matrix dislocation structures into PSBs during the fatigue in copper single crystals /36/. It was found that a sudden change in the amplitude of cyclic deformation generates ladder structures similar to those shown in Fig. 1, and the aperiodicity of the ladder (with dislocation-rich walls and dislocation-poor channels) diminishes if one waits for a long enough time. This means that at last an aperiodic ladder structure relaxes to a periodic one.

All these modulated structures are unobtainable from the linear stability analysis. However, we show that they can be reasonably well described using the concept of the Eckhaus instability which was successfully applied earlier in the theory of convection, in the studies of current-carrying states in narrow superconducting channels, and in hydrodynamics. The Eckhaus instability is connected with the dynamics of the wavelength-changing process. In one of the stages of this process, aperiodic long-living transients (which appear via nonlinear interactions) relax to a periodic structure. This is exactly what one observes in the TEM experiments. At present we consider only quasi-one-dimensional systems. Such a simplified approach is justified by the TEM observations which show that the evolution of quasi-one-dimensional PSBs is nearly independent of changes in the surrounding matrix structure /35/.

We start with the WA-model for a coupled system of two populations of dislocations (mobile and relatively immobile). The Eckhaus instability then is studied by using the nonlinear amplitude

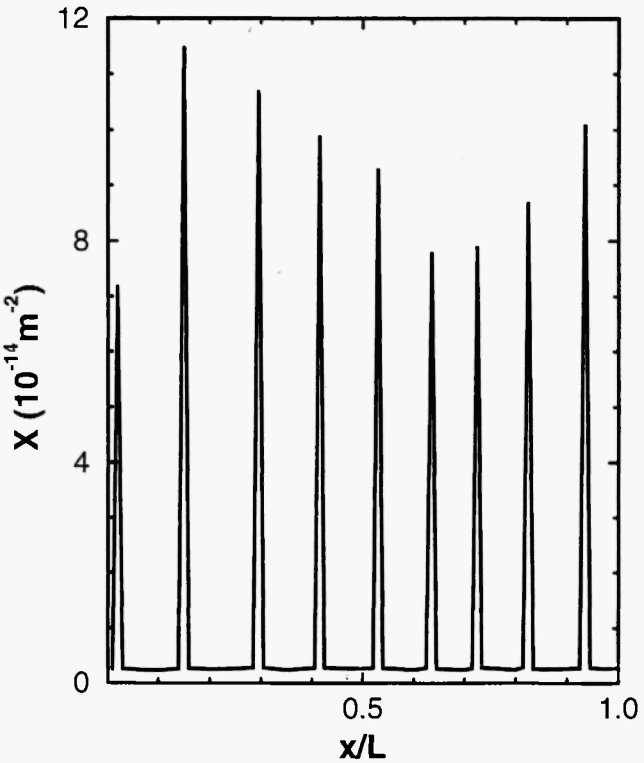

Fig. 2: The density of immobile dislocations, X, as a function of scaled length, x/L, for a one-dimensional "grain" (grain size L = 13 μm) obtained in numerical simulations by Glazov and Laird /34/. The final-size analog of the WA-model was used, the modulated structure persists for a very long time.

(Ginzburg-Landau) equation which can be derived from the WA-model in the vicinity of a continuous pattern-forming instability, i.e., in the regime of weak nonlinearity. Recently, the same approach based on the GL equation was adopted by Salazar *et al.* /37/ for the analysis of spatio-temporal dislocation patterns. They found "unexpected solutions" in the form of spiral waves and concluded, on this basis, that an approach based on the GL equations is limited. In this paper we are not going to analyze all possible spatio-temporal patterns which can be obtained within the framework of the GL approach. Instead, we concentrate on looking for the steady-state spatial waves of dislocation densities. For this purpose we use the GL equation for the soft mode instability which describes the formation of dislocation patterns and their spatial modulations, instead of the GL equation for the hard mode (which describes unstable modes rapidly changing with time) used in Ref. /37/. Thus the GL equation obtained for the soft mode does not contain any "unphysical" solutions.

The paper is organized as follows. The WA-model for a coupled system of two dislocation populations and its linear stability analysis are briefly reviewed in Sec. II. Section III contains the derivation of the GL equation for the soft mode which describes steady-state spatial patterns (see also

Appendix A). We show that the values of all the coefficients of the GL equation for the soft mode are real. We estimate these coefficients for the values of parameters describing a realistic dislocation system. Sec. IV contains a qualitative description of the process of the Eckhaus instability formation and development.

A detailed analysis of the dynamics of the wavelength-changing process and the relation between the Eckhaus instability and experimentally observed modulated dislocation patterns are discussed in Sec. V. In general, the wavelength-changing process is very complicated, especially in the case where an unstable initial wave vector is close to the Eckhaus stability limit. However, the hierarchy of relaxation rates for different modes can generate a metastable phase modulated pattern which survives for a long time before transition into the final (Eckhaus stable) pattern occurs. We discuss the scenario of appearance of metastable modulated patterns in real experimental conditions.

A conclusion and summary of the results are presented in Sec. VI.

II. THE WALGRAEF-AIFANTIS MODEL AND ITS LINEAR STABILITY

Following the WA-model /1,2/ we have a system of two coupled equations for the densities of mobile (n_2) and immobile (n_1) dislocations in the following form:

$$\begin{aligned} \frac{\partial n_1}{\partial t} &= g(n_1) - bn_1 + \gamma n_1^2 n_2 + D_1 \frac{\partial^2 n_1}{\partial x^2}, \\ \frac{\partial n_2}{\partial t} &= bn_1 - \gamma n_1^2 n_2 + D_2 \frac{\partial^2 n_2}{\partial x^2}. \end{aligned} \tag{1}$$

Here D_1 and D_2 are the "generalized mobility" coefficients of the immobile and mobile dislocations ($D_1 \ll D_2$), respectively, b and γ characterize the freeing of immobile dislocations and the nonlinear interaction between dislocations. $g(n_1) = \alpha - \beta n_1^2$ is the source function which describes the multiplication of dislocations, e.g., by means of the Frank-Read proeess /10,11/ (and represented by the constant term α), and the annihilation of dislocations with opposite Burgers vectors (parameter β, all the constants are real and positive).

Of course, such a description is very approximate and ignores several important factors. First, the multiplication term α which represents the Frank-Read process is assumed to be a constant. However, it must obviously depend on the coordinates and on time and also contain information about the reaction of the system on the local stress state, i.e., to be fluctuating. Second, the constants b and γ describe the "local" interactions between dislocations only and ignore any long-range forces between dislocations. Third, the diffusion ("generalized mobility") process may also depend on the local environment of a given dislocation, i.e., the model of diffusion in a homogeneous medium with a constant diffusion coefficient may be inadequate (the diffusive nature of dislocation mobility can be strictly justified only for some special mechanisms such as, e.g., double cross-slip mechanism). Also,

the cubic nonlinearity in the governing equations has been critically discussed in the literature (see, e.g., Ref. /17/). Therefore, this model is approximate and qualitative. Nevertheless, it is its simplicity which allows us to understand analytically some features of dislocation patterning, and this feature makes the model particularly attractive.

Using the standard procedure described, for example, in Ref. /38/, we represent the densities n_1 and n_2 as

$$n_1 = n_1^c + q_1,$$
$$n_2 = n_2^c + q_2, \tag{2}$$

where n_0^1 and n_2^0 are the steady-state solutions of Eq. (1),

$$n_1^0 = \left(\frac{\alpha}{\beta}\right)^{1/2},$$
$$n_2^0 = \frac{b}{\gamma}\left(\frac{\beta}{\alpha}\right)^{1/2}. \tag{3}$$

Eq. (1) then can be rewritten as

$$\dot{\mathbf{q}} = \hat{L}\mathbf{q} + \mathbf{f}(\mathbf{q}), \tag{4}$$

where q is the vector,

$$\mathbf{q} = \begin{pmatrix} q_1(x,t) \\ q_2(x,t) \end{pmatrix}, \tag{5}$$

$\hat{L}$ is the linear operator,

$$\hat{L} = \begin{pmatrix} (b-b_0) + D_1\frac{\partial^2}{\partial x^2} & a \\ -b & -a + D_2\frac{\partial^2}{\partial x^2} \end{pmatrix}, \tag{6}$$

and the vector f(q) contains all the nonlinear terms,

$$\mathbf{f}(\mathbf{q}) = \begin{pmatrix} f_1(x,t) \\ f_2(x,t) \end{pmatrix} = \begin{pmatrix} (d-\beta)q_1^2 + cq_1q_2 + \gamma q_1^2 q_2 \\ -dq_1^2 - cq_1q_2 - \gamma q_1^2 q_2 \end{pmatrix}. \tag{7}$$

The parameters a, b, c, d are defined as

$$\begin{aligned} a &= \gamma(n_1^0)^2 = \frac{\gamma\alpha}{\beta}, \\ b_0 &= 2\sqrt{\alpha\beta}, \\ c &= 2\gamma n_1^0 = 2\gamma\sqrt{\frac{\alpha}{\beta}}, \\ d &= \gamma n_2^0 = b\sqrt{\frac{\beta}{\alpha}}. \end{aligned} \tag{8}$$

The difference between the WA-model and the classical "brusselator" model used for studying the kinetics of chemical reactions (see, e.g., Refs. /38-40/) is the presence of an additional quadratic non-linear term describing the annihilation process of two dislocations with opposite Burgers vectors.

We start with linear stability analysis and assume the solution to have the form

$$\mathbf{q}(x,t) = \mathbf{q}_0 \exp(\lambda_k t) \exp(ikx). \tag{9}$$

Using Eq. (4) we find

$$\lambda = \frac{\tilde{\alpha}}{2} \pm \frac{1}{2}\sqrt{\tilde{\alpha}^2 - 4\tilde{\beta}}. \tag{10}$$

where

$$\begin{aligned} \tilde{\alpha} &= -D_1^k - D_2^k + (b - b_0) - a, \\ \tilde{\beta} &= (D_1^k - (b - b_0)) \cdot (D_2^k + a) + ab, \end{aligned} \tag{11}$$

and $D_1^k = D_1 \cdot k^2, D_2^k = D_2 \cdot k^2$.

There are several control parameters which can create instability in the system. Below it is assumed that we change the freeing parameter b and consider all other parameters as constants. Instability occurs when one of the two eigenvalues of Eq. (10) becomes positive at some wave vector k. We are interested in steady-state spatial patterning, i.e., in the case where the discriminant in Eq. (10) is not negative. One can easily check that the soft mode instability first occurs at a nonzero wave vector,

$$k_c^2 = \sqrt{\frac{b_0 a}{D_1 D_2}}, \tag{12}$$

when the freeing parameter b becomes equal to its critical value,

$$b = b_c = \frac{1}{D_2}\left[(D_2 b_0 + D_1 a) + 2\sqrt{(D_2 b_0) \cdot (D_1 a)}\right]. \tag{13}$$

Defining a new parameter, $\mu = \sqrt{D_1 / D_2} \ll 1$, one gets

$$b_c = (\sqrt{b_0} + \mu\sqrt{a})^2. \tag{14}$$

Most of these derivations are standard and not original (see, e.g., Refs. /1,2,39/ for a similar analysis). They are presented here in order to facilitate understanding of the following material.

III. GINZBURG-LANDAU EQUATION FOR THE SOFT MODE

We derive the Ginzburg-Landau equation for the soft mode using the standard procedure (see, e.g., Refs. /38,41/). It is assumed that the solution q(x,t) has the form

$$\mathrm{q}(x,t) = \sum_{j,k} \xi_{j,k}(x,t)\mathrm{q}_{j,k} \exp(ikx), \tag{15}$$

where the summation is made over all the wave vectors k and over the number of eigenvector j at a given k. ξ is supposed to be a slowly varying function of coordinate (in comparison with $\exp(ik_c x)$). Because the undamped modes (with $\lambda > 0$) may grow unlimited provided the nonlinear terms in Eq. 4 are ignored, the amplitudes of these modes are bigger than those of the damped modes. On the other hand, near the "phase transition" point the relaxation time for the undamped modes tends to infinity, i.e., the damped modes must adiabatically follow the undamped ones. Although the amplitudes of the damped modes are small, they must not be neglected completely. The equations for the damped modes which follow from such a "slaving principle" are usually just algebraic equations that can be easily solved. (Here we discuss the case of the soft mode instability only. For the hard mode one has to take into account time oscillations of the unstable modes.) Inserting q(x,t) from Eq. (15) into Eq. (4) and dividing all the modes (j,k) into stable and unstable ones, we get the GL equation for the soft mode (a detailed derivation is presented in Appendix A):

$$\dot{\xi} = (\lambda_0 + \lambda_2 \cdot \nabla^2)\xi - B|\xi|^2\xi, \tag{16}$$

where $\xi(x,t)$ describes the unstable mode with $\lambda > 0$ (at the wave vector $k = k_c$), and the coefficients λ_0, λ_2, and B are defined as

$$\begin{aligned}
\lambda_0 &= (b - b_c)\frac{\sqrt{b_0 a}}{(1-\mu^2)(\sqrt{b_0 a} + a\mu)} + O\left[(b-b_c)^2\right], \\
\lambda_2 &= \frac{8\mu(b_0 a)}{(1-\mu^2)(\sqrt{b_0 a} + a\mu)k_c^2}, \\
B &= \frac{8}{9\mu\sqrt{b_0 a}}\left[\gamma b_c - \beta^2\left(\frac{b_c}{\sqrt{\alpha\beta}} - 1\right)^2\right].
\end{aligned} \tag{17}$$

The coefficient λ_0 disappears at $b = b_c$, defining the point of the "phase transition", i.e., the value of b at which the bifurcation occurs, and a spatial periodic structure develops. The coefficients λ_0 and λ_2 were calculated exactly, i.e., taking into account all the orders of the parameter μ. When calculating the coefficient B we kept only the term of the order of $1/\mu$ which dominates in the only case interesting to us ($\mu \ll 1$).

We notice that the values of all the coefficients in the GL equation are real. This result coincides with those obtained earlier for a similar "brusselator" model (see, e.g., Ref. /38/). Analogous results were obtained in Ref. /42/ where the formation of spatial patterns on planar continua was considered, and real values of the coefficients in the GL equations followed from the necessity for the dynamics to commute with some symmetry operations. The GL equation with real coefficients cannot exhibit solutions in the form of spiral waves studied in Ref. /37/, where the GL equation with complex coefficients describing the hard mode instability (the unstable mode is oscillating in time) was used. We were rather interested in spatial patterning only, i.e., we used the equation for the soft mode. We would like to emphasize that the analysis of all possible spatio-temporal patterns in dislocation systems was not the goal of the present publication, and for studies of steady-state spatial patterns the GL equation for the soft mode seems to be completely adequate.

The next interesting feature of Eq. (16) is a critical dependence of the coefficient B on the parameter γ which describes the cubic nonlinearity in the WA-model. When $\gamma < \gamma_c$,

$$\gamma_c = \frac{\beta^2}{b_c}\left(\frac{b_c}{\sqrt{\alpha\beta}} - 1\right)^2, \tag{18}$$

the coefficient B becomes negative, and a nonzero space- and time-independent solution of the GL equation disappears. In a general case, the change of the sign of the cubic term means that the cubic GL equation is not sufficient, and higher order terms must be properly taken into account (i.e., one gets a transition from a supercritical to a subcritical bifurcation regime). The detailed analysis of different bifurcational behavior could be performed using the power series expansion approach described, e.g., in Ref. /41/, and recently used in Ref. /43/ for analysis of limit cycle solutions in a model similar to ours (it is based on equations for three different types of dislocation densities but considers only the time-dependent part and neglects the spatial coupling). We are not doing such a general analysis here because for realistic values of the parameters we always have $\gamma \gg \gamma_c$ (see below), the coefficient B is large and positive, and we do expect that the bifurcation forming the onset of the periodic pattern is supercritical.

For further study of a continuous pattern-forming instability in the vicinity of the threshold, it is convenient to change the units and variables (see, e.g., Refs. /44,45/), namely, the part of the sum of Eq. (15) which corresponds to the undamped modes can be written as

$$\mathbf{q}(x,t) = \varepsilon^{1/2} \cdot \chi \cdot \left[\mathbf{q}_{u,k_c} \cdot A(X,T)e^{ik_c x} + c.c.\right] = \varepsilon^{1/2} \cdot \chi \cdot \left[\mathbf{q}_{u,k_c} \cdot \Phi + c.c.\right], \tag{19}$$

where $\varepsilon = (b - b_c)/b_c$ measures the distance from the threshold. $X = \sqrt{\varepsilon}x/\xi_0$ and $T = \varepsilon t/\tau_0$ are slow space and time variables, and *c.c.* denotes the complex conjugate. $\mathbf{q}_{u,k_c}$ is the eigenvector for the unstable mode (see Appendix A); the function $\Phi - A(X,T)\cdot \exp(ik_c x)$ describes a slow modulation of the periodic basic solution. This function defines all the spatial and temporal changes of the order parameter $\mathbf{q}(x,t)$. Following Ref. /44/ we generated the real valued order parameter $\mathbf{q}$ for steady-state pattern (for which the instability happens simultaneously on both the wave vectors k_c and $-k_c$). χ is an additional parameter,

$$\chi = \sqrt{\frac{9\mu\sqrt{b_0 a}}{8(\gamma - \gamma_c)}}, \tag{20}$$

which formally contains a singularity at $\gamma = \gamma_c$. Actually, this singularity does not create any real problem because one always has $\gamma \gg \gamma_c$ for a realistic set of parameters of the system (see below). ξ_0 and τ_0 are the relaxation time and the coherence length,

$$\begin{aligned} \tau_0 &\simeq \frac{1}{\dot{b}_c}, \\ \xi_0^2 &= \frac{8\sqrt{b_0 a}}{b_c}\frac{\mu}{k_c^2}. \end{aligned} \tag{21}$$

The amplitude $A(X, T)$ satisfies the standard dimensionless GL equation,

$$\partial_T A = \nabla_X^2 A + A(1 - |A|^2). \tag{22}$$

It can be seen that $\mathbf{q}(x, t)$ is proportional to $\sqrt{\mu}$ at small values of μ. This means that the patterning formation process does not develop in a dislocation system where "immobile" dislocations cannot diffuse at all ($\mu = 0$).

The periodic stationary solutions of Eq. (22) above the threshold exist only for $Q^2 < 1$,

$$A = a_0 e^{iQX}, a_0 = \sqrt{1 - Q^2}, \tag{23}$$

and the solution with a given Q corresponds to the wavenumber

$$k = k_c + \frac{\varepsilon^{1/2} Q}{\xi_0} = k_c \cdot \left(1 + \varepsilon^{1/2}\sqrt{\frac{b_c}{8\mu\sqrt{b_0 a}}} \cdot Q\right). \tag{24}$$

For further numerical estimations we use the set of parameters recommended by Schiller and Walgraef /46/ and used in Ref. /34/: time was measured in fatigue cycles, *cy* (this is a natural time unit for cyclic mechanical testing; further we assume that the frequency of cyclic testing is of the order of one cycle per second, which is quite realistic); $\hat{a} = 6\ \text{cy}^{-1}$; $\hat{b} = 30\ \text{cy}^{-1}$; $\hat{c} = 200\ \text{cy}^{-1}$; $D_1 = 3\times10^{-15}\ \text{m}^2\cdot\text{cy}^{-1}$;

$D_2 = 4 \times 10^{-11}$ m^2·cy^{-1}. Here $\hat{a}$, $\hat{b}$, and $\hat{c}$ are related to our parameters as

$$\begin{aligned} \hat{a} &= 2\beta n_1^0 - b_0 \\ \hat{c} &= \gamma (n_1^0)^2 = a \\ \hat{b} &= \hat{c} \cdot \frac{n_2^0}{n_1^0} = b, \end{aligned} \tag{25}$$

and $\mu = \sqrt{D_1 / D_2} \sim 10^{-2}$, i.e., $\mu \ll 1$. We obtain $\lambda_c = 2\pi/k_c = 0.7$ μm, which seems in agreement with experiment (see, e.g., Refs. /34,35/ and Figure 1); $\gamma_c/\gamma = \hat{a}/4\hat{c} \ll 1$, i.e., we can neglect the parameter γ_c in comparison with γ in Eq. (20). For this set of parameters, Eq. (24) can be rewritten as

$$k = k_c \cdot (1 + 1.7\varepsilon^{1/2} Q). \tag{26}$$

The parameter χ in Eq. (19) is small ($\chi \sim 0.05 \cdot n_1^0$), which is much smaller than the density of immobile dislocations at the stationary point. This means that our approach based on the GL equation describes the behavior of the system only in the vicinity of the bifurcation point.

In this work we chose the parameter b as a control parameter of the system, i.e., we considered the behavior of the system just above the critical value of this parameter, $b_c \approx b_0 = \hat{a} = 6$ cy^{-1}. If we compare this value with $b = \hat{b} = 30$ cy^{-1}, chosen in Ref. /34/ for numerical simulations, we see that the realistic system is very far from the bifurcation point, i.e., our present consideration of a weakly nonlinear system is quite qualitative. However, it provides a clear physical interpretation of spatial aperiodicity of dislocation patterns observed experimentally.

IV. THE ECKHAUS INSTABILITY AND APERIODICITY OF PATTERNS

Continuous systems with spatially periodic stationary solutions are of interest in various physical and chemical systems /47,48/. From Eqs. (23) and (24) one can easily see that the onset of periodic patterning is defined by the neutral curve $\varepsilon = \xi_0^2 (k - k_c)^2$ (which corresponds to $|Q| = 1$). Below this curve a periodic solution with an infinitesimally small amplitude will decay, i.e., this curve defines the linear stability region. However, inside the linear stability curve, the periodic pattern can become unstable through the development of slow spatial modulations of the periodic structure if the vector Q is larger than the so-called Eckhaus stability limit ($Q_E = 1/\sqrt{3} \approx 0.5574$ for small ε) /32/. After some evolutional period, the system ends at the periodic state with the new wavenumber $Q < Q_E$. The Eckhaus instability is a very important mechanism of patterns selection which can significantly change the wavenumber of the pattern. Experimentally it can be observed, e.g., by quenching the system into an unstable wavenumber and observing its subsequent transition into a stable Q-state (see, e.g., Ref. /49/, where the onset of thermal convection in a thin fluid was experimentally observed).

The modulations of the periodic structure can be described by introducing the "longitudinal phase diffusion coefficient" which becomes negative for an unstable solution, thus defining a wavenumber-changing process. The total set of nonlinear equations for a slowly varying phase in a one-dimensional reaction-diffusion system (in the fully nonlinear region) was obtained by Kramer and Zimmerman /44/. However, this general approach is not very convenient for practical simulations, and the physics of the wavelength-changing process can be better understood in the weakly nonlinear regime, i.e., near the GL threshold.

There exist two general approaches to qualitative description of the Eckhaus instability. The first of them is based on an analysis of the static solutions of Eq. (22) which can be obtained by writing $A(X, T)$ in terms of real amplitude $R(X, T)$ and phase $\Theta(X, T)$ functions /44,50-52/,

$$A = R\exp(i\Theta). \tag{27}$$

Then the stationary solutions satisfy the condition $J = const$, where $J = R^2\partial_X\Theta$ is the integral of motion, and the equation for R can be written in a form analogous to Newton's equation of motion for the particle in some potential $U(R)$, which is monotonic for $J^2 > J_c^2 = 4/27$, and has a maximum and a minimum (i.e., a bounded solution can exist) for $J^2 < J_c^2$. The spatially periodic solutions are stable for wave vectors $Q^2 < Q_E^2 = 1/3$, and unstable for $Q^2 > Q_E^2$.

In addition to the periodic solutions one gets a class of solutions with periodically modulated R (and $\partial_X\Theta$). They correspond to saddle-points of the Ginzburg-Landau functional, can be expressed in terms of elliptic integrals, and are unstable (see, e.g., Refs. /51,52/). These solutions correspond to the most interesting case of a wavelength-changing process. However, they can be expressed in tractable form only when the two roots of the cubic polynomial in the denominator of the elliptic integral coincide (i.e., the modulation vector K is zero) /44,51,52/. This situation has been discussed earlier for current-carrying superconductors /52/ and for systems with Rayleigh-Benard instability /51/.

An alternative way of considering the Eckhaus instability is the secondary linear stability analysis of the solution of Eq. (22) with an unstable wave vector Q ($Q^2 > 1/3$) /50/. The maximal growth rate (σ_{max}) of the destabilizing "Eckhaus modes" is exhibited at the modulation vector K_{max} (the new wave-numbers of the system are $Q \pm K_{max}$),

$$\begin{aligned} \sigma_{max} &= (3Q^2 - 1)^2/4Q^2, \\ K_{max}^2 &= (3Q^2 - 1)(Q^2 + 1)/4Q^2. \end{aligned} \tag{28}$$

Numerical simulations for a system which consists of a single mode with an Eckhaus-unstable Q and an additional broad band random noise of small amplitude /50/ show that, in general, this scenario is true, and after competition between different modes only one Fourier component with the wave vector near $Q - K_{max}$ survives in the final state. If the system is very close to the Eckhaus stability limit, the

wavenumber-changing process becomes very complicated, and the system ends up at some stage with $Q - \alpha K_{max}$, where $0 < \alpha < 1$.

Before the system gets into the final state with an Eckhaus stable wavelength, it goes through intermediate states containing many harmonics, and the instantaneous spatial shape of the pattern at these moments should be studied numerically.

V. NUMERICAL RESULTS AND DISCUSSION

Following Ref. /50/ we do numerical simulations for the system which is initialized in a state with several periodic modes of the form

$$A(X,0) = a_0(0)e^{iQX} + \sum_{m=N_{min}}^{N_{max}} a_m(0)e^{iX(Q+mK)}, \tag{29}$$

where N_{min} and N_{max} are the minimal and the maximal numbers of modes considered, Q is the initial (Eckhaus unstable) wave vector, K is the vector characterizing the change of the wavelength. If the initial vector Q is far from the Eckhaus stability limit, Q_E, the vector K can be taken near the value of K_{max} for a given Q (see previous section), and the number of modes that should be taken into account is small. If the wave vector Q is close to Q_E, the process becomes very complicated and includes many harmonics. In such a case one has to perform numerical simulation with a small value of K and a large number of modes, and the coefficients $a_m(0)$ should be considered as small random perturbations.

The time evolution of the coefficients $a_m(T)$ is given by the GL equation

$$\begin{aligned} \partial_T a_m &= \Omega_m a_m - \sum_{k,l} a_k a_l a^*_{k+l-m}, \\ \Omega_m &= 1 - (Q + mK)^2. \end{aligned} \tag{30}$$

The coefficients a_m can be taken as real, and $A(X, T)$ is an almost periodic function of X at a fixed T.

The evolution of the system consists of two main stages. In the first one (the "branching stage"), modes with wavenumbers Q and mK appear and grow via nonlinear interactions. In the second ("selection") stage, all the side branches disappear, except the only final mode. These processes are illustrated in Fig. 3 for two different sets of $a_m(0)$'s. The initial unstable wave vector (Q = 0.6) was close to the Eckhaus stability limit, the value K = 0.025 was taken for both examples, 41 modes were taken into account (N_{min} = -20, N_{max} = +20), and $a_0(0) = \sqrt{1-Q^2} + 0.1$. Eq. (30) was integrated numerically using the fourth-order Runge-Kutta method. Further increase in the number of modes does not change the result significantly. For each set of the initial conditions, the system develops slowly and smoothly ("branching") before a certain moment where many harmonics start to grow fast, and after an intermediate stage of intensive competition between several modes, the system selects one mode which saturates in time, while others die out. However, evolution of the system is complicated

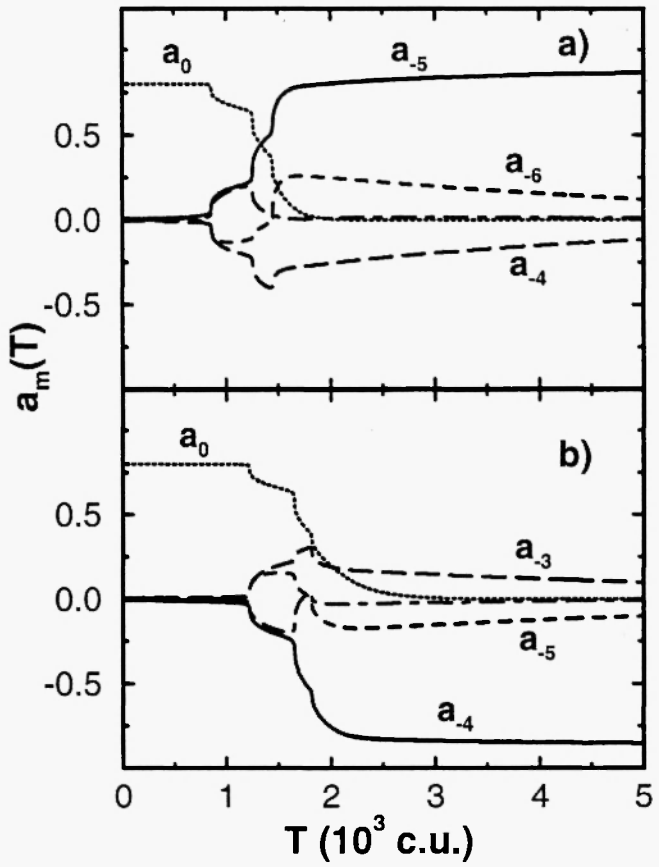

Fig. 3: Time evolution of the coefficients $a_m(T)$ (only a few modes with largest amplitude are drawn). $Q = 0.6$, $K = 0.025$, 41 modes, $a_0(0) = (1 - Q^2)^{0.5} + 0.1$. The perturbation at the moment $T = 0$ was taken in the form $a_m(0) = 0.01 \cdot (-1)^{m+1}$ where $m = -5,\ldots,-1$, for the (a) – part of the Figure and $m = -4,\ldots,-1$ for the (b) – part. All the other coefficients $a_m(0)$ were equal to zero. Time T is measured in the conventional units (c.u.) used in the standard dimensionless GL equation (see previous sections).

and is defined by a number of separatrices /50/. The initial conditions for Fig. 3a) and b) are very similar but the evolution processes (and the final saturated mode) are different. Here we are not going to perform any detailed investigation of separatrices and regions of attraction for this system.

Most important for our consideration is the fact that, in both cases, in addition to the saturated mode ($m = -5$, for the upper part of Figure 3), there are two "satellites" ($m = -6$ and $m = -4$) which are dying very slowly in time and, therefore, can generate the modulated structure of the pattern in the real space which persists for a long time. Here we considered the case where the "selection stage" takes a long time, which is quite usual if Q is close enough to Q_E. In some cases we observed a long "branching stage" where several modes with comparable amplitudes develop slowly in time due to nonlinear

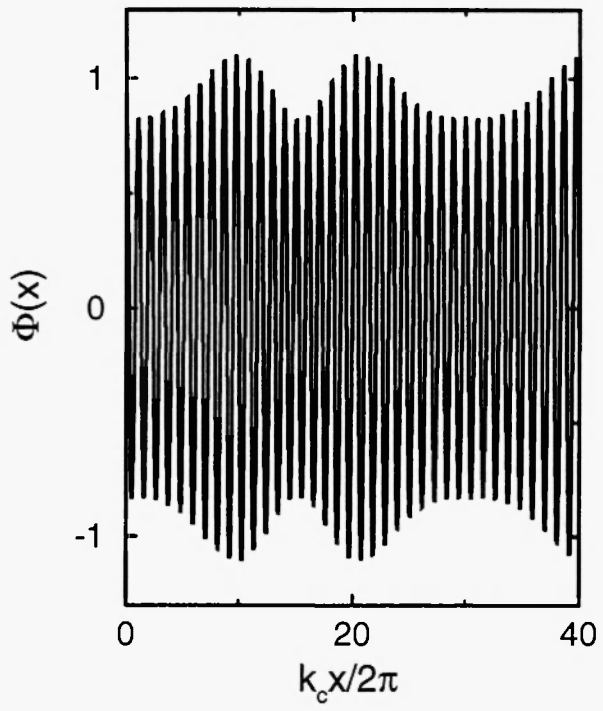

Fig. 4: The "order parameter" $\Phi(x)$ at a certain moment during the "selection stage" as a function of a "dimensionless coordinate", $k_c x/2\pi$, for the system with $Q = 0.6$, $K = 0.01$, 101 modes, and $a_0(0) = (1 - Q^2)^{0.5} + 0.1$. The initial values of the other coefficients $a_m(0)$ were taken randomly from the interval between –0.01 and 0.01, $\varepsilon = 0.3$.

interactions. However, this is rather an exception than a typical behavior. Figure 4 provides an example of a typical behavior of the function $\Phi(x)$ (see Eq. (19)) which contains all the information about spatial and temporal changes of the order parameter $q(x, t)$ (we consider only the real part of the function Φ which we will call the "order parameter"). The behavior of Φ obviously exhibits an amplitude modulation of the undisturbed periodic function (with the wave vector k_c). A fragment of the same Figure drawn in another scale shows that phase modulation also takes place in the system (Fig. 5). In the presence of phase modulation, the distance between the neighboring maxima of the dislocation density changes with the spatial coordinate (Figure 7). Note that the distance between the maxima is not chaotic – it exhibits a nearly periodic behavior with the period much larger than unity (the unity corresponds to the main period of the undisturbed system, $2\pi/k_c$). The shape of the curve is quite universal – a simple linear transformation of coordinates makes any two curves (which correspond to different values of ε) equivalent. Such a behavior is also obvious from Eq. (26).

In Figure 6 we show a two-dimensional plot of the order parameter (one coordinate is a dummy) which is similar to the experimentally observed ladder structure of PSBs shown in Fig. 1. The absolute values of the phase modulation in our simulations for a weakly nonlinear system are somewhat smaller

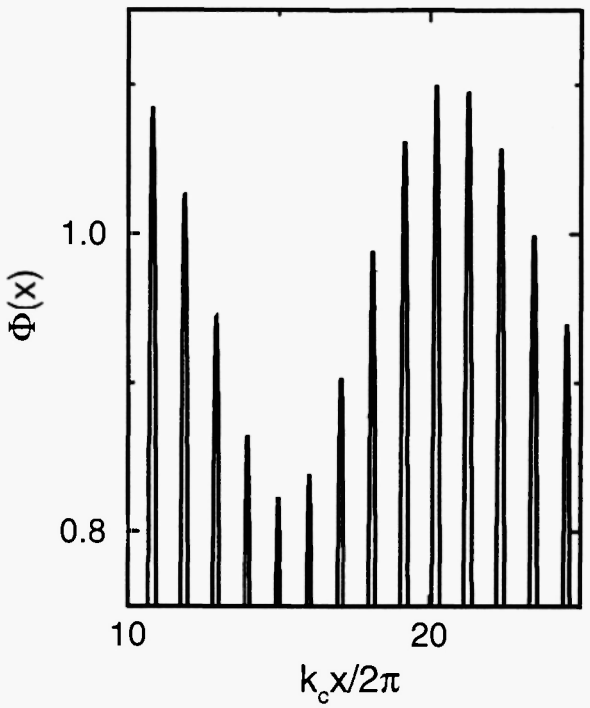

Fig. 5: The fragment of the curve of Fig. 4 shown in other coordinates.

than the experimental ones. The direct numerical calculations of dislocation densities in the fully nonlinear system (far from the bifurcation threshold) by Glazov and Laird /34/ give the values of modulation which are closer to experiment (Fig. 2). However, the theoretical analysis of the results obtained from numerical simulations in Ref. /34/ was restricted to linear stability analysis, and the reason for the appearance of these modulations has not been highlighted.

In the examples considered above, the time T was measured in conventional units (c.u.) used in the dimensionless GL equation. Let us assume that the lifetime of a metastable modulated structure (ΔT, the time interval during which we can consider the structure nearly unchanged) is of the order of 3000 c.u. (which is quite realistic for $Q = 0.6$, see Figure 3). This corresponds to $\Delta T/\varepsilon b_c = 6000$ cy ~ 6000 seconds ~ 1.5 hour, for $\varepsilon = 0.1$ (we assumed as before that the frequency of the cyclic testing is of the order of one cycle per second). This means that modulated structures for a given Q can persist at least for hours. When Q approaches Q_E, the lifetime of the metastable modulated structure grows as $1/(Q-Q_E)^2$, i.e., it has no upper bound.

From the above analysis one can easily imagine the scenario of appearance of such modulated structures in fatigued crystals. If there exists some pattern with the wave vector Q which is stable for a given set of the parameters of the system, this pattern can become unstable at the next moment when some of the parameters suddenly change their values. The pattern starts to change its wavelength and, if Q is close to Q_E, this process can generate a long-living metastable structure. In the numerical examples

Fig. 6: The two-dimensional plot of $\Phi(x, y)$. The coordinate y is a "dummy", and the x-dependence of $\Phi(x, y)$ corresponds to $\Phi(x)$ shown in Figure 5.

considered above, we illustrated how such a wavelength-changing process can produce modulated structures in a weakly nonlinear system.

A qualitatively similar behavior has been observed in recent very accurate studies of the TEM images, where the time evolution of the distance between the dislocation-rich walls in PSBs has been statistically analyzed /35/. It was shown that the statistical distribution of the distance between the two

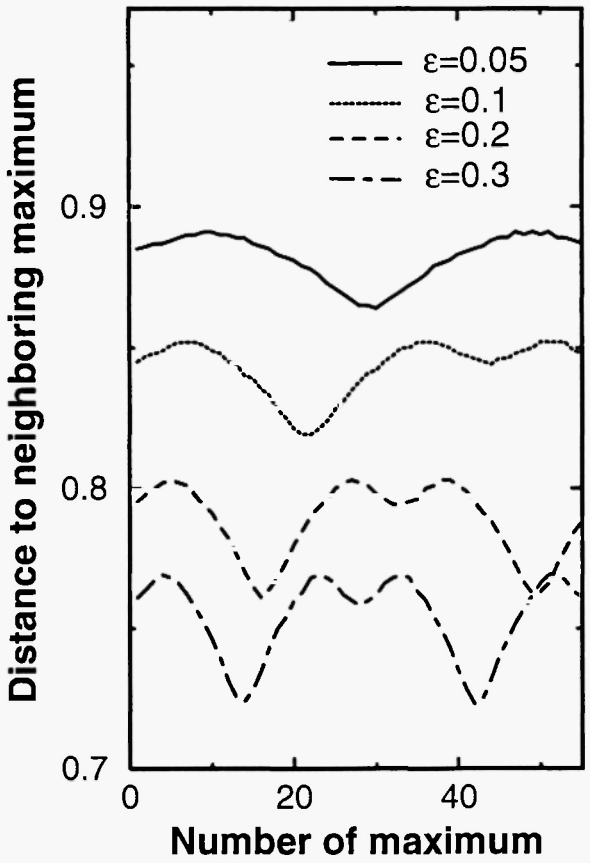

Fig. 7: The distance between the nearest maxima as a function of the number of maximum for the order parameter $\Phi(x)$ shown in Figure 4 (for different values of ε).

nearest walls is very asymmetric at the moment when the PSBs have just been generated from the initial matrix structure by a sudden change in the cyclic loading amplitude (actually, the asymmetric PSBs appear very fast; this corresponds to the fast "branching stage" when different modes develop via nonlinear interactions). If the cyclic loading regime is no longer changing, this aperiodic structure exhibits the tendency to become periodic, i.e., the distribution function of the dislocation wall spacings becomes narrower in time. This means that the wavelength-changing process evolves in time to some final periodic structure through certain stages that contain intermediate long-living transients. Such a behavior is very similar to that for the Eckhaus instability.

The real experimental situation is, of course, much more complicated than that described by the WA-model. The only justification for application of this model to dislocation dynamics is based on some similarities of the behavior of densed dislocation systems and the kinetics of chemical reactions. Then, the evolution of the real system takes place under the cyclic loading conditions. The effects of the cyclically changed applied stress are not taken directly into account in the WA-equations, and the

dislocation structures in a real crystal will not evolve without the presence of stress in the system (the diffusion motion is closely connected with fluctuations of the local stress).

However, the experiment shows that the most important period of evolution coincides with the first quarter of the first cycle with a suddenly increased amplitude. The flow stress at this moment reaches its maximal high value, and the density of mobile dislocations grows fast because of decoupling of the edge dislocation dipoles /35/. This means that the amplitude of the cyclic deformation plays the role of the freeing parameter b in the WA-model which controls the transformation of immobile dislocations into mobile ones. Also, our model assumes that the permanent presence of an external cyclic loading generates a fluctuating stress field inside the sample, and this field supports the diffusive motion of dislocations. The sudden change of the parameter b in the system can also initiate a possible wavelength-changing process. Therefore, the experimental situation is quite similar to the evolutional behavior of the Eckhaus instability, namely, (i) after a change in the control parameter, the system makes a fast transition into a very aperiodic pattern ("branching"); (ii) this pattern evolves to the new stable periodic state through an intermediate long-living transient ("selection").

This similarity makes it possible to consider the Eckhaus instability as a "generic" mechanism that plays an important role in real dislocation systems. This mechanism might be one of the fundamental processes that "probes" the topological stability of a given dislocation pattern and may result in its modulations and subsequent structural rearrangements (e.g., vein structure → ladder structure of PSBs → mazes → cells, etc.).

VI. CONCLUSIONS

In this paper we made an attempt to understand qualitatively the nature of modulated dislocation structures in fatigued metals which were observed in TEM experiments (see Refs. /33,35/). We demonstrated that these modulations can be qualitatively explained using the concept of the Eckhaus instability /32,44,45,50/. A detailed quantitative theory which describes the dynamics of the wavelength-changing process does not yet exist, and one has to do computer simulations for every particular system. We tried to illustrate how such simulations can help to understand modulated ladder dislocation patterns and some universality of their behavior.

We considered quasi-periodic one-dimensional ladder structures in cyclically deformed metals. The question of application of the Eckhaus instability theory to more realistic two- or three-dimensional systems is still open. At least we know that in the two-dimensional extended anisotropic systems the nature of Eckhaus instability remains essentially unchanged /49,53/. However, during the wavelength-changing process some defects may appear /54/. Also, an approach based on the Ginzburg-Landau equations and analysis of their instabilities in the parametric space seems to be a powerful tool for studying the spatial patterns and their transformations in continuous planar systems /42/. We believe that the concepts of Eckhaus instability, phase modulations and wavenumber-changing

processes, represent one of the fundamental mechanisms of dynamic dislocation structure rearrangements which governs the topological stability of dislocation patterns.

Also, it would be a great challenge to understand whether the presence of random and periodic external forces in the system can change the stable solutions of the GL equations, i.e., how the presence of "white" or "colored" noise in the system changes the pattern selection mechanisms. Random forces are always present in dislocation systems, and if the pattern selection process depends on noise, the behavior of the system should be similar to those numerous physical, chemical, and biological systems where noise-induced transitions were predicted theoretically and observed experimentally /26-28,38,40, 55,56/. The presence of an external periodic force corresponds to taking of the cyclic loading into direct consideration (i.e., a more exact model than those considered above). This study would be extremely important for practical applications. Recent numerical simulations of different regimes of cyclic deformation in metallic alloys based on nonlinear dynamics show that the cyclic loading can generate a variety of different temporal dissipative structures /57/. However, to the best of our knowledge, the effects of spatial coupling in such a system have never been studied theoretically or by means of numerical simulations.

ACKNOWLEDGMENTS

This work was supported by the Alcoa Foundation Grant, and this support is gratefully acknowledged.

APPENDIX A: DERIVATION OF THE GL EQUATION

In this Appendix we derive Eq. (16). Following the recommendations of Refs. /38,41/, we divide all the modes of Eq. (15) into stable (s) and unstable (u) modes,

$$\mathrm{q}(x,t) = \sum_{u,k} \xi_{u,k}(x,t)\mathrm{q}_{u,k} \exp(ikx) + \sum_{s,k} \xi_{s,k}(x,t)\mathrm{q}_{s,k} \exp(ikx). \qquad \text{(A1)}$$

In the one-dimensional case there are only two possible unstable modes, (u, k_c) and ($\tilde{u}$, $-k_c$). They correspond to instabilities at the two wave vectors with the same absolute value but opposite directions.

The linear term in Eq. (16) describes the bifurcation behavior of the order parameter for unstable modes when the value of b exceeds b_c. Taking into account Eq. (10) for the eigenvalue of the unstable mode, and considering $(b - b_c)$ as a small parameter, one easily gets the result for λ_0 in Eq. (17).

The term containing the spatial gradient appears from the separation of slow and fast varying spatial variables. Namely, we suppose that $\xi_{u,k_c}(x, t)$ is varying in space much slower than exp (ik_cx). Then all the gradient terms can be extracted from the k-dependence of λ near the point $k = k_c$. Assuming that $k =$

$k_c + q$ (q is small), we are looking for the coefficients λ_1 and λ'_2 of the expression

$$\lambda(q) = \lambda_0 + \lambda_1 \cdot q + \lambda'_2 \cdot q^2, \tag{A2}$$

where

$$\lambda_1 = 0,$$
$$\lambda'_2 = -\frac{8\mu(b_0 a)}{(1-\mu^2)(\sqrt{b_0 a} + a\mu)k_c^2}. \tag{A3}$$

In the real space, q corresponds to $1/i \cdot \partial/\partial x$, i.e., we get $\lambda_2 = -\lambda'_2$, for λ_2 in Eq. (16).

For the contributions from nonlinear terms we have to substitute $q(x, t)$ into Eq. (7). Following Ref. /38/, we suppose that the stable modes (s, k) are at least of the order of the square of (u, k). At first, we notice that in the equation for the unstable mode (e.g., (u, k) = (u, k_c)) there will be no contribution from the nonlinearity of the type (u', k') ·(u'', k''). Each term of that type must be multiplied by the factor $\delta(k' + k'' - k)$, which is obtained from the integral of the product of three exponents. Each of the wave vectors k, k', and k'' must have the value $+k_c$ or $-k_c$, i.e., the δ-function is always zero except for the non-interesting case of $k_c = 0$. Therefore, one has to keep only terms of the type (u', k') ·(s'', k'') (further we denote the collection of these terms by the symbol $F^{(2)}$), or (u', k') ·(u'', k'')·(u''', k''') (denoted as $F^{(3)}$). Both $F^{(2)}$ and $F^{(3)}$ are of the cubic order of (u, k).

Simple calculations show that

$$F^{(3)} = \frac{\gamma}{L}\int_{-L/2}^{L/2} dx \phi_1^*(x)\phi_{k'}(x)\phi_{k''}(x)\phi_{k'''}(x) \cdot \xi_{u',k'}\xi_{u'',k''}\xi_{u''',k'''} \times$$
$$\times \left(q^{(1)}_{u,k}, q^{(2)}_{u,k}\right) \cdot \begin{pmatrix} q^{(1)}_{u',k'} q^{(1)}_{u'',k''} q^{(2)}_{u''',k'''} \\ -q^{(1)}_{u',k'} q^{(1)}_{u'',k''} q^{(2)}_{u''',k'''} \end{pmatrix}, \tag{A4}$$

where the length L is considered to be large in comparison with $1/k_c$, but small in comparison with the characteristic length scale of the change in ξ, q and $\bar{q}$ are the right and left eigenvectors (the column and the line) of the linear operator given by Eq. (6), $\phi_k(x) = exp(ikx)$. This immediately gives

$$F^{(3)} = 3\gamma \cdot (\bar{q}_1 - \bar{q}_2) \cdot q_1^2 q_2 \cdot |\xi|^2 \xi, \tag{A5}$$

where we denote $k = k_c$, $\xi = \xi_{u,k}$, $q_i = q^{(i)}_{u,k}$, and $\bar{q}_i = \bar{q}^{(i)}_{u,k}$ (i = 1, 2) for brevity.

For calculations of $F^{(2)}$ we use the slaving principle which gives simple equations for $\xi_{s,k}$. We easily see that only the stable modes with vectors $k = 0$ and $k = 2k_c$ have to be taken into account, i.e.,

$$F^{(2)} = (-2)\cdot(\bar{q}_1,\bar{q}_2)\cdot\begin{pmatrix}(d-\beta)q_1+\frac{1}{2}cq_2, & \frac{1}{2}cq_1\\ -dq_1-\frac{1}{2}cq_2, & -\frac{1}{2}cq_1\end{pmatrix}\cdot\begin{pmatrix}(d-\beta)q_1+cq_2\\ -dq_1-cq_2\end{pmatrix}\cdot q_1\times$$
$$\times\sum_s\left(\frac{2}{\lambda_{s,0}}+\frac{1}{\lambda_{s,2k_c}}\right)\cdot|\xi|^2\xi, \qquad \text{(A6)}$$

where $\lambda_{s,0}$ and $\lambda_{s,2k_c}$ are both negative.

The right and left eigenvectors for the unstable mode can be chosen, e.g., in the form

$$\begin{pmatrix}q_1\\ q_2\end{pmatrix} = \begin{pmatrix}1\\ -\mu\left(\mu+\sqrt{\frac{b_0}{a}}\right)\end{pmatrix},$$
$$(\bar{q}_1,q_2) = \left(\frac{1}{1-\mu^2},\frac{\mu}{(1-\mu^2)\left(\sqrt{\frac{b_0}{a}}+\mu\right)}\right). \qquad \text{(A7)}$$

The resulting equations for $F^{(2)}$ and $F^{(3)}$ can be significantly simplified in the most interesting case of $\mu \ll 1$. Then $F^{(2)} = O(\mu)$, and in Eq. (A6) one has to keep only the eigenvalue at $k = 2{\cdot}k_c$ (which is of the order of μ, others are $O(1)$). Then for the coefficient B in Eq. (16) we get:

$$B = \frac{8}{9\mu\sqrt{b_0 a}}\left[(d-\beta)^2-\frac{cd}{2}\right] = \frac{8}{9\mu\sqrt{b_0 a}}\left[\gamma b_c-\beta^2\left(\frac{b_c}{\sqrt{\alpha\beta}}-1\right)^2\right]. \qquad \text{(A8)}$$

REFERENCES

1. D. Walgraef and E.A. Aifantis, *Int. J. Engng. Sci.*, **23**, 1351 (1985).
2. D. Walgraef and E.A. Aifantis, *Int. J. Engng. Sci.*, **24**, 1789 (1986).
3. D.J. Bammann and E.A. Aifantis, *Acta Mechanica*, **44**, 259 (1982).
4. E.A. Aifantis, in: *Defect Fracture and Fatigue*, G.C. Sih and J.W. Provan (Eds.), Martinus Nijhoff, 1983; p. 75.
5. E.A. Aifantis, *Transactions of ASME, J. Engng. Mat. Tech.*, **106**, 326 (1984).
6. E.A. Aifantis, in: *Dislocations in Solids*, H. Suzuki, T. Ninomiya, K. Sumino and S. Takeuchi (Eds.), Tokyo University Press, Tokyo, 1985; p. 41.
7. D. Walgraef and E.A. Aifantis, *J. Appl. Phys.*, **58**, 688 (1985).
8. E.A. Aifantis, *Mater. Sci. Eng.*, **81**, 563 (1986).
9. E.A. Aifantis, *Int. J. Plasticity*, **3**, 211 (1987).
10. J.P. Hirth and J. Lothe, *Theory of Dislocations*, John Wiley & Sons Inc., New York, 1982.

11. F.R.N. Nabarro, *Theory of Crystal Dislocations*, Dover Publications Inc., New York, 1987.
12. V. Vitek, in: *Stability of Materials*, A. Gonis, P.E.A. Turchi and J. Kudrnovsky (Eds.), Plenum Press, New York, 1996; p. 53.
13. V.V. Bulatov, S. Yip and A. Argon, *Phil. Mag.*, **A72**, 453 (1995).
14. A. Seeger, in: *Dislocations 1984*, P. Veyssiere, L.P. Kubin and J. Castaing (Eds.), CNRS, Paris, 1984; p. 141.
15. M.S. Duesberry and Z.S. Basinski, *Acta Metall. Mater.*, **41**, 643 (1993).
16. V. Bulatov, F.F. Abraham, L.P. Kubin, B. Devincre and S. Yip, *Nature* (in press, 1999).
17. L.P. Kubin and G. Canova, *Scripta Metall. Mater.*, **27**, 957 (1992).
18. B. Devincre, P. Veyssiere, L.P. Kubin and G. Saada, *Phil. Mag.*, **A75**, 1263 (1997).
19. H.M. Zbib, M. Rhee and J.P. Hirth, MME Report No. 96-21, WSU, 1996.
20. Y. Brechet, G. Canova and L.P. Kubin, *Acta Metall. Mater.*, **44**, 4261 (1996).
21. L.P. Kubin, in: *Computer Simulations in Materials Science*, H.O. Kirchner *et al.* (Eds.), IBM, Netherlands, 1996; p. 273.
22. L.P. Kubin, in: *Materials Science and Technology: A Comprehensive Treatment*, R.W. Cahn, P. Haasen and E.J. Kramer (Eds.), VCH, Weinheim, 1993; p. 138.
23. G. Ananthakrishna and M.C. Valsakumar, *J. Phys. D: Appl. Phys.*, **15**, L171 (1982).
24. G. Ananthakrishna and D. Sahoo, *J. Phys. D: Appl. Phys.*, **14**, 2081 (1981).
25. G. Ananthakrishna, *Scripta Metall. Mater.*, **29**, 1183 (1993).
26. M. Zaiser and P. Hähner, *Phil. Mag. Lett.*, **73**, 369 (1996).
27. P. Hähner, *Appl. Phys.*, **A63**, 45 (1996).
28. M. Zaiser, *Acta Mater.* (in press, 1999).
29. E.A. Aifantis, *J. Mech. Behav. Mater.*, **5**, 355 (1994).
30. E.A. Aifantis, *Int. J. Eng. Sci.*, **33**, 2161 (1995).
31. T.B. Benjamin and J.E. Fair, *J. Fluid Mech.*, 27, 417 (1966); J.T. Stuart and R.C. DiPrima, *Proc. Roy. Soc. London A*, **362**, 27 (1978).
32. W. Eckhaus, *Studies in Non-Linear Stability Theory*, Springer, New York, 1965.
33. C. Lair, P. Charsley and H. Mughrabi, *Mater. Sci. Engineering*, **81**, 465 (1986).
34. M.V. Glazov and C. Laird, *Acta Metall. Mater.*, **43**, 2849 (1995).
35. U. Holzwarth and U. Essmann, *Appl. Phys.*, **A57**, 131 (1993).
36. The authors would like to express their sincere gratitude to Dr. Michael Zaiser who drew our attention to this paper.
37. J.M. Salazar, R. Fournet and N. Banai, *Acta Metall. Mater.*, **43**, 1127 (1995).
38. H. Haken, *Synergetics*, Springer-Verlag, Berlin, 1978.
39. G. Nicolis and I. Prigogine, *Self-Organization in Non-Equilibrium Systems (from Dissipative Structures to Order through Fluctuations)*, Wiley, New York, 1977.
40. I. Prigogine and L. Lefever, *J. Chem. Phys.*, 48, 1695 (1968).
41. H. Haken, *Advanced Synergetics*, Springer-Verlag, 1983.

42. G.H. Gunaratne, *Phys. Rev. Lett.*, **71**, 1367 (1993).
43. M. Bekele and G. Ananthakrishna, *Phys. Rev.*, **E56**, 6917 (1997).
44. L. Kramer and W. Zimmermann, *Physica D*, **16**, 221 (1985).
45. B. Janiaud, A. Pumir, D. Bensimon, V. Croquette, H. Richter and L. Kramer, *Physica D*, **55**, 269 (1992).
46. C. Schiller and D. Walgraef, *Acta Metall. Mater.*, **36**, 563 (1988).
47. P.C. Hohenberg and J.S. Langer, *J. Stat. Phys.*, 28, 193 (1982).
48. J.E. Wesfreid and S. Zaleski (Eds.), *Cellular Structures in Instabilities*, Springer, New York, 1984.
49. M. Low and J.P. Gollub, *Phys. Rev. Lett.*, **55**, 2575 (1985).
50. L. Kramer, H.R. Schober and W. Zimmermann, *Physica D*, **31**, 212 (1988).
51. A.C. Newell and J.A. Whitehead, *J. Fluid Mech.*, **38**, 279 (1969).
52. J.S. Langer and V. Ambegaokar, *Phys. Rev.*, **164**, 498 (1967).
53. S. Rasenat, E. Braun and V. Steinberg, *Phys. Rev.*, **A43**, 5728 (1991).
54. W. Pesch and L. Kramer, *Z. Phys. B*, **63**, 121 (1986).
55. W. Horsthemke and R. Lefever, *Noise-Induced Transitions*, Springer, Berlin, 1984.
56. J. Honekamp, *Stochastic Dynamic Systems*, VCH, Weinheim, 1990.
57. M.V. Glazov, D.R. Williams and C. Laird, *Appl. Phys. A*, 64, 373 (1997).

SELF-ORGANIZATION, DISLOCATION – POINT-DEFECT INTERACTIONS, AND INSTABILITIES IN FATIGUE

A. Seeger *

Department of Physics, University of Cape Town
Rondebosch 7700
South Africa

(Received December, 1997)

ABSTRACT

The paper develops a theory of cyclic hardening and formation of persistent slip bands in fatigue based on simultaneous and coupled self-organization processes of dislocations and intrinsic atomic defects (vacant lattice sites and atoms in lattice interstices). The relationships between three dichotomies, viz. thermodynamic reversibility–irreversibility, and inversive–non-inversive and conservative–non-conservative dislocation motion, as well as their rôles in the structure formation by self-organization are discussed in detail. An "abstract" model for the hardening in cyclic deformation is presented. It postulates the existence of two distinct hardening mechanisms, one of them (called "obstacle mechanism") being strongly strain-rate and temperature dependent and building up gradually with increasing cumulative plastic strain. This model accounts well not only for the cyclic hardening but also for the main features of the cyclic stress–strain curve and of the persistent slip bands, including the stability properties of the microstructure under changes of the temperature of deformation.

A "realization" of the abstract hardening model in terms of mechanisms is proposed. It involves the generation of atomic defects by the moving dislocations, the clustering of atomic defects as a result of generalizations of the Lück–Sizmann mechanism, and the destruction and dispersion of the clusters (the "obstacles" of the abstract theory) when cut by moving dislocations.

In an Appendix it is shown that not only are the dependences of the residual electrical resistivity of fatigued copper crystals on the cumulative plastic strain and on the annealing temperature in full accord with the proposed hardening mechanisms but that they can provide complementary information in addition. The relevance of annealing data for the understanding of the properties of self-interstitials in fcc metals is discussed.

1. INTRODUCTION

Face-centred cubic (fcc) metals undergoing fatigue, i.e., being subjected to large numbers of small-amplitude stress–strain cycles, are perfect examples of highly dissipative systems capable of

* Permanent address: Max-Planck-Institut für Metallforschung, Heisenbergstraße I, D-70569 Stuttgart, Germany.

self-organization[1]. For definiteness let us consider an fcc single crystal, say of copper, orientated for single glide in a <110> {111} glide system and subjected to alternating uniaxial strain ("push–pull"). The resolved shear stress in the glide system is denoted by σ, the corresponding total shear strain (elastic plus plastic) by ε, the resolved plastic shear strain by ε_{pl}, the resolved plastic shear-strain rate by $\dot{\varepsilon}_{pl}$, and the amplitude of the resolved cyclic plastic shear strain by $\hat{\varepsilon}_{pl}$. As a measure of the total glide undergone by the specimen the so-called *cumulative plastic strain*

$$\varepsilon_{pl,cum} := 4N\hat{\varepsilon}_{pl} \tag{1}$$

is used, where N denotes the number of cycles. (Here and later, the symbol := means "defined as".) The area enclosed by a loop in the σ–ε plane,

$$w_\varepsilon = \oint \sigma d\varepsilon = \oint \sigma(\varepsilon_{pl}) d\varepsilon_{pl} \quad , \tag{2}$$

is the net mechanical work per unit volume done on the specimen during one cycle.

A particularly well-defined way to perform cyclic deformation experiments is to keep $|\dot{\varepsilon}_{pl}|$, $\hat{\varepsilon}_{pl}$, and the temperature T fixed /2,3/. The mean of the absolute values of the external resolved shear stresses reached in two consecutive half cycles,

$$\hat{\sigma} := \left[\sigma(\hat{\varepsilon}_{pl}) - \sigma(-\hat{\varepsilon}_{pl})\right]/2, \tag{3}$$

is denoted as *peak stress*. The relationship between $\hat{\sigma}$ and the cumulative plastic strain [defined by (1)], $\hat{\sigma} = \hat{\sigma}(\varepsilon_{pl\,cum})$, is called the *cyclic-hardening curve*. In the context of hardening, $\hat{\sigma}$ is often referred to as *flow stress* in order to emphasize the close relationship to the flow stress in uniaxial plastic deformation [2].

The shape of the $\sigma - \varepsilon_{pl}$ loops changes gradually with increasing N ($dw_\varepsilon/dN > 0$) until, under the conditions just mentioned, it remains constant within experimental accuracy (see, e.g., /2/). This corresponds to a plateau in the cyclic-hardening curve (cf. Fig. A1 in the Appendix). The peak stress in this "saturation regime" is called the *saturation stress* and is denoted by $\hat{\sigma}_{sat}$. As the cyclic deformation continues, on a time scale large compared to the inverse cycling frequency the fatigue specimen is in a quasi-stationary state. In the saturation regime it constitutes an open system in which virtually the entire free energy supplied from outside (the mechanical work performed by the push–

---

[1] For a general discussion of the rôle of self-organization processes and of irreversible thermodynamics in crystal plasticity the reader is referred to "Thermodynamics of Open Systems, Self-organization, and Crystal Plasticity" /1/. According to the classification given there, the irreversible processes responsible for the self-organization in crystal plasticity have to be classified as "evolutionary".

[2] The peak stress has been defined by (3) rather than by $\sigma(\hat{\varepsilon}_{pl})$ in order to eliminate or at least minimize the effects of asymmetries in tension and compression. These may have their origin in a push–pull asymmetry of the experimental set-up or in an asymmetry of the glide mechanism (as, e.g., in the case of glide on {211} planes in body-centred cubic (bcc) metals /4/).

pull machine) is dissipated. The qualification "virtually" alludes to the fact that although within experimental accuracy the shape of the $\sigma - \varepsilon_{pl}$ loops and thus w_ε remain constant, there must be structural changes going on (a tiny fraction of w_ε presumably being *stored* in the specimen in the form of additional lattice defects) as evidenced by the fact that with increasing N fatigue cracks begin to develop, whose growth eventually results in the rupture of the specimen.

According to the seminal work of Ilja Prigogine on "dissipative structures", the conditions in the saturation regime of cyclic deformation described in the preceding paragraph are ideal for self-organization to occur or, rather, for such structures to be the outcome of self-organization processes. This suggests strongly that the most prominent microstructural feature in the saturation regime, the so-called *persistent slip bands* [3] (PSBs), are formed by self-organization processes. As the electron micrograph Fig. 1 shows by way of example, in the microstructure of the saturation regime of cyclically deformed fcc metals there is indeed considerable order, particularly inside the PSBs, which exhibit a ladder-like arrangement of screw dislocations. We shall return to the topic of self-organization after considering the relationship between the so-called cyclic stress–strain curve and PSB formation.

The *cyclic stress–strain curve* is the relationship between the saturation stress, $\hat{\sigma}_{sat}$, and the plastic-strain amplitude, $\hat{\varepsilon}_{pl}$. In fcc metals it has a very characteristic shape (Fig. 2), in which three regimes may be discerned, conventionally denoted by A, B, C /2/. The clarification of the relationship between PSB formation and the three regimes of the cyclic stress–strain curve is mainly due to Winter /5,6/. In regime A there are no PSBs at all, in B matrix (as the PSB-free part of the crystal will be called) and PSBs coexist (cf. Fig. 1), while in C the crystal is completely filled with PSBs. Winter /5/ discovered that in regime B the volume fraction occupied by PSBs, f_{PSB}, varied linearly with the strain amplitude $\hat{\varepsilon}_{pl}$, a result that was subsequently verified by Mughrabi /2/ with greater accuracy. From this result it was deduced that once PSBs are formed, the cyclic plastic deformation is essentially confined to them (in other words: PSBs are soft, the matrix is hard, the strain amplitude in the PSBs being by about a factor of 10^2 larger than in the matrix) and that under given conditions of temperature and strain rate the cyclic deformation in the PSBs takes place with a fairly well-defined strain amplitude $\hat{\varepsilon}_{PSB}$. According to this interpretation, $\hat{\varepsilon}_{PSB}$ can be read off from the cyclic stress–strain curve at the transition between the regimes B and C (see Fig.2). The corresponding stress amplitude, σ_{PSB}, coincides with the saturation stress $\hat{\sigma}_{sat}$ in regime B.

Winter /5/ noted that the relationship between the saturation stress, $\hat{\sigma}_{sat}$, and the strain amplitude, $\hat{\varepsilon}_{pl}$, is, to some extent, analogous to that between pressure and density of a fluid. At low pressures the fluid is in the vapour state. When the fluid is compressed, at a certain pressure (in the analogy corresponding to σ_{PSB}) the pressure ceases to increase. A second phase, the liquid, is formed. Only

[3] The name "*persistent slip bands*" has its origin in the fact that in optical microscopy of polished surfaces the PSBs look like "ordinary" slip bands. Whereas these are steps generated by dislocations that have left the crystal and that can therefore be removed by polishing, the persistent slip bands are bulk features that "persist" when the crystal surface is polished after the cyclic deformation.

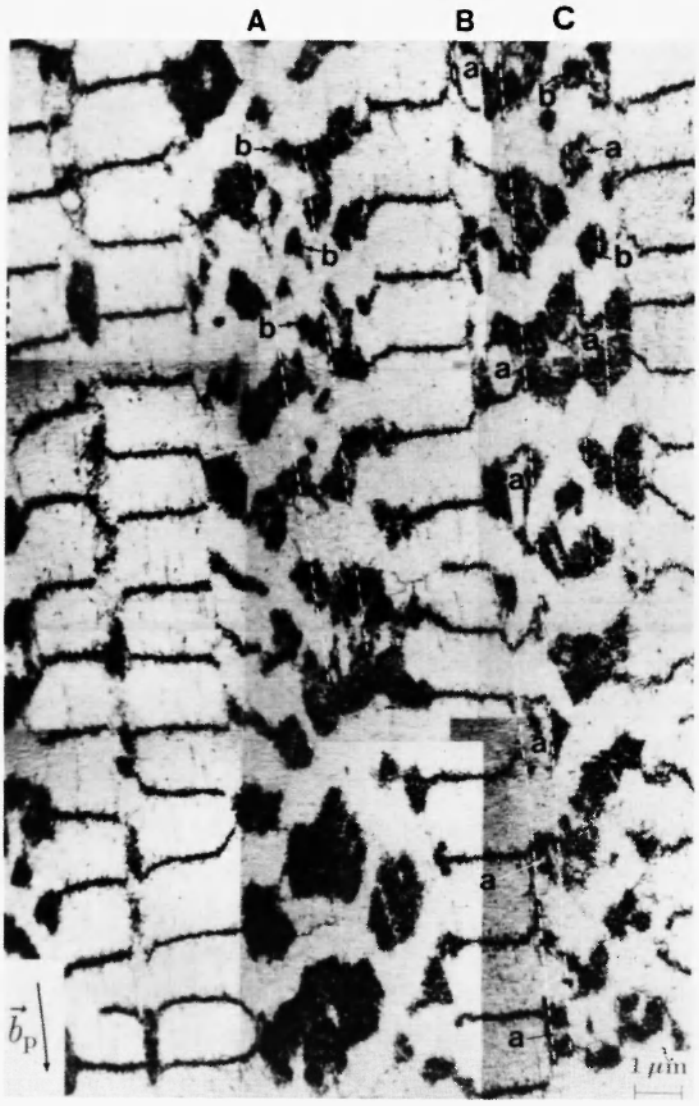

Fig. 1: Transmission electron micrograph of a $(1\bar{2}1)$ section of a copper single crystal cyclically deformed at 300 K to saturation ($\hat{\varepsilon}_{pl} = 2.2 \cdot 10^{-3}$). Before the preparation of the section the crystal was irradiated with fast neutrons in order to fix the dislocation pattern. $\vec{b}_p = (10\bar{1})$ denotes the Burgers vector of the primary glide system; the diffraction vector was $(20\bar{2})$. The regions with the quasi-regular ladder structure are persistent slip bands; the faint lines parallel to $\vec{b}_p$ between the rungs are screw dislocations. A, B, C denote incipient persistent slip bands developing inside the matrix. The letter a denotes regions of low dislocation densities that have developed inside the matrix at approximately constant separations. Examples of regions of higher-than-average dislocation density developing with approximately constant separations are indicated by the letter b. (Courtesy of U. Holzwarth /3/.)

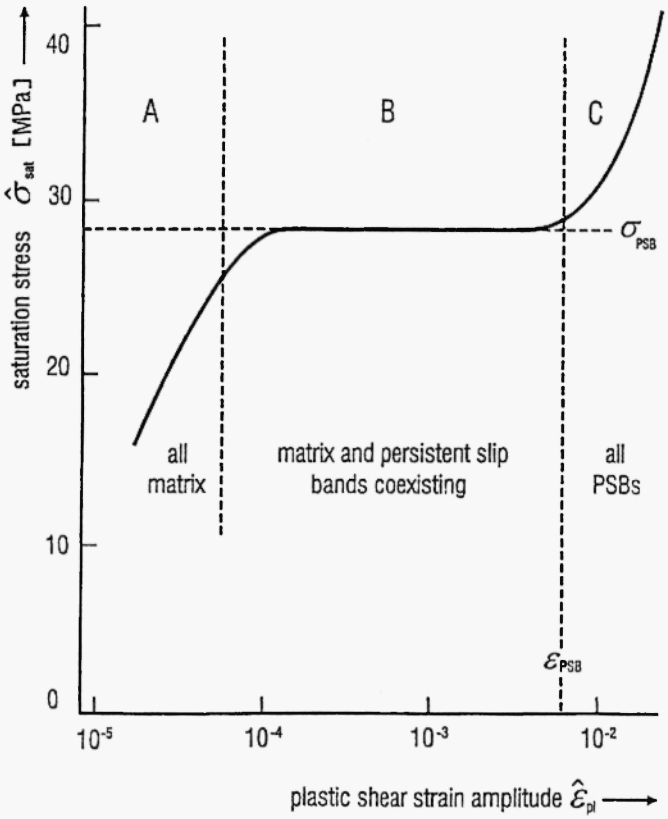

Fig. 2: Cyclic stress–strain curve of Cu single crystals orientated for single glide. The numerical values pertain to room-temperature deformation /2/.

when, upon further compression, the entire fluid has been transformed into liquid does the pressure rise again. In Winter's analogy the density at which this occurs corresponds to ε_{PSB} .

The analogy between Winter's "two-phase model" of low-amplitude fatigue and the vapour–liquid transition is incomplete in several respects, however, and should therefore be used with prudence. The most important deviation was noted by Winter himself /5/: Whereas the vapour–liquid transition is reversible (i.e., essentially the same pressure–density relationship is followed during compression and dilation), the $\hat{\sigma}_{sat}(\hat{\varepsilon}_{pl})$ relationship is not. When $\hat{\varepsilon}_{pl}$ is reduced, only a small fraction of the PSBs become inactive, contrary to what is expected from the analogy /5/. Furthermore, the rôles of the soft (PSBs, vapour) and hard (matrix, liquid) phases are interchanged in the two cases. With regard to the influence of temperature the analogy does hold: The density at which vapour and liquid coexist and ε_{PSB} have in common that with increasing temperature they decrease until above a certain temperature (the critical temperature of the liquid; in the case of fatigue a "critical temperature" that is presumably determined by the frequency of cross-slip, as will be argued below) there is only one "phase" left.

About a decade ago, Seeger and Frank /7/ proposed a model for the formation of persistent slip bands based on the concept that the PSBs are indeed *dissipative structures* resulting from the *self-organization of dislocations*. The present paper describes an extension of this model. It follows closely a lecture course given by the author at the Universität Stuttgart during the winter term 1989/90. The main ingredients of the model to be presented are the following:

(*i*) Dislocations and atomic defects (vacancies and self-interstitials) [4] undergo *simultaneous* and *coupled* self-organization processes.

(*ii*) The structure formation in cyclic deformation is mainly due to what may be called *generalized Lück–Sizmann effect*. They involve the *mutual annihilation* of defects (dislocations or atomic defects) of *opposite* sign and the *clustering* of defects of the *same* sign. (Self-interstitials and vacancies are considered to be defects of opposite sign; so are dislocations with opposite Burgers vectors.)

(*iii*) The coupling between the self-organization processes of dislocations and atomic defects comes about, on the one hand, by the clusters of atomic defects (later on simply called defect clusters) acting as *obstacles* for the dislocation movement and, on the other hand, by the participation of dislocations in both the *build-up* and the *destruction* of the defect clusters.

(*iv*) The dislocation motion is restricted to essentially *two dimensions* (glide on one of the {111} glide planes, plus occasional climb accompanied by the emission or absorption of vacancies or self-interstitials). This is analogous to the rôle played by the one-dimensional migration of crowdions in the formation of void lattices during the radiation damage of metals at elevated temperatures /8/.

According to (*iv*), cross-slip of screw dislocations, which permits the dislocations to move in *three* dimensions, opposes the formation of persistent slip bands. In fcc metal crystals orientated for single glide, the onset of extensive cross-slip is presumably the reason why the formation of persistent slip bands ceases at elevated temperatures /7/. (In crystals orientated for double glide, additional mechanisms may play a rôle /9/.) Since in the fec structure there is an intimate relationship between stacking-fault energy and cross-slip /10/, this suggestion may be tested by systematic experiments on the temperature dependence of the formation of persistent slip bands in fcc metals [5].

The present paper is organized as follows. Sect. 2 deals with general aspects of dislocation motion and their relationships to thermodynamic irreversibility. In the discussion of the dislocation motion

---

[4] We prefer the denotation "atomic defects" to the widespread expression "point defects" used in the title of this paper, since the most important feature of "point defects" is that they are *not* 'points' but have properties such as volume or crystallographic symmetry incompatible with 'points', and that often they may take up different crystallographic orientations.

[5] The hypothesis that cross-slip prevents the formation of PSBs explains immediately why PSBs and the mechanical properties going with them are not found in body-centred cubic metals /7/. Here the onsets of cross-slip and of extensive plastic deformation coincide /11/. The fact that the softening phenomena associated with PSBs, to be discussed in Sect. 3, are absent in bcc metals is the experimental basis for the so-called cyclic-deformation technique (also known as Mughrabi–Ackermann technique) for determining the strain-rate and temperature dependence of the flow–stress of bcc metals /4,12/.

the dichotomies "inversive–non-inversive" and "conservative–non-conservative" will be emphasized. Sect. 3 considers the hardening associated with low-amplitude plastic deformation of fcc metals in terms of phenomenological concepts. In Sect. 4 the discussion of cyclic hardening is carried further, now considering specific mechanisms. It will be seen that the interplay between dislocation motion on the one hand and the nucleation, growth, and destruction of clusters of atomic defects forming obstacles for the dislocation motion on the other hand is crucial for the understanding of cyclic hardening. The information gained in this respect from studies of the residual electrical resistivity, which in metals is a sensitive measure of dispersed (in contradistinction to clustered) atomic defects, is treated in the Appendix. The main conclusions of the paper are summarized in Sect. 5. As the reader will notice, the presentation maintains to some extent the pedagogical style of the lecture course referred to above. It is emphasized that the present paper is *not* meant to be a review of the *literature* on the subject.

2. CLASSIFICATIONS OF DISLOCATION MOTIONS

By definition, *plastic deformation* of a solid requires that, after removing the load, a *permanent* deformation (usually somewhat smaller than the plastic deformation under load) will remain on the time scale of observation. From the point of view of thermodynamics, plastic deformation is a highly irreversible process. Only rarely remains more than a few percent of the net mechanical work done during plastic deformation stored in the deformed samples in the form of lattice defects, such as dislocations, twin boundaries, or atomic defects. Most of the free energy supplied from outside through the deformation equipment is transformed into heat. If during the plastic deformation isothermal conditions are maintained, the dissipated free energy is transferred to the heat bath. It is the large "entropy export" connected with this that allows self-organization processes during plastic deformation to take place /1,7/ [6]. As mentioned in Sect. 1, in the saturation regime of fatigue the fraction of mechanical free energy *not* dissipated is, in fact, unmeasurably small.

Let us now look at permanent deformations from the point of view of dislocation movements. (We exclude, for the time being, cases in which the plastic deformation is *not* due to dislocation motion.) A permanent deformation can result only if the locations of the dislocations after unloading are *not* the same as before the loading. This implies that the unloading paths (in a two-dimensional sense, meaning the areas swept out by the dislocations) have to be different from the loading paths. It is

[6] Self-organization processes play indeed a major rôle in all modes of plastic deformation involving high densities of dislocations. This is in contrast to the view that the dislocation patterns resulting from plastic deformation may be understood in terms of "minimal energy". Trivially, the energy of the dislocation arrangements found after unloading is a *local* minimum with respect to *small* glide movements, but the *absolute* minimum is, of course, the dislocation-free crystal.

tempting to call "kinematically reversible" those cyclic deformations in which the loading and unloading paths of the dislocation coincide, and "kinematically irreversible" those in which they differ. However, since – as we shall see presently – "kinematic reversibility" implies thermodynamic reversibility only rarely, it was felt that a different nomenclature should be used. It is proposed that dislocation movements in which loading and unloading path are the same be called '*inversive*', those in which this is not the case '*non-inversive*'.

As a simple example illustrating the preceding, consider Fig. 3. A dislocation line anchored in its glide plane vibrates under the action of a small alternating shear stress. The area swept out by the dislocation, indicated by hatching, is the same in both directions of motion; hence the motion is *inversive*. Whether it is *reversible* (in the sense of thermodynamics) or not depends on the circumstances. If the motion is frictionless and in phase with the cyclic external stress, there is no energy dissipation, hence the process (which under these conditions is quasi-static) is thermodynamically reversible. In this case the σ–ε diagram is a line passing through the origin. Experimentally, this is a limiting situation which may be approximately realized in highly perfect crystals if both the amplitude and the frequency of the applied stress are small. In general, however, the dislocation motion is *not* frictionless, e.g., owing to electron and/or phonon drag. This leads to energy dissipation. In the stationary state of cyclic straining the σ–ε diagram then is a closed loop with finite opening, and the integral (2) becomes positive (cf. the right-hand side of Fig. 3). Note that electron and phonon drag are just two of quite a number of processes that make inversive dislocation motion thermodynamically irreversible. In the terminology introduced by Zener /13/, in all these cases the deformations resulting from inversive dislocation motion have to be classified as "anelastic" [7].

If in the situation pictured on the left-hand side of Fig. 3 the stress amplitude is more and more increased, the Frank–Read mechanism of sending out dislocation loops will begin to operate /14/. The loops will reach the crystal surface (forming slip lines and slip bands), react with other dislocations (e.g., by mutual annihilation), undergo cross-slip, leave their glide-planes by climb, etc. It is therefore

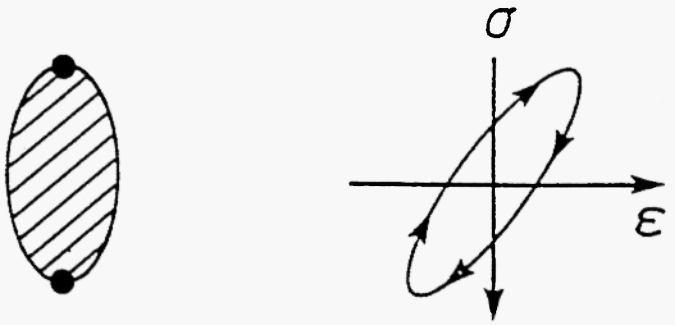

Fig. 3: Dislocation line vibrating between two anchoring points, with stress–strain diagram.

[7] In his classical work, Zener /13/ did *not* consider dislocations, however.

extremely unlikely that after unloading the original dislocation pattern will be restored even approximately; hence the crystal has now undergone permanent ("plastic") deformation [8].

The preceding example shows the importance of non-inversive dislocation motion for achieving permanent deformation. We now consider some of these non-inversive processes in more detail.

If dislocations of opposite sign *meet on the same glide plane*, they will attract each other and annihilate. This process is clearly non-inversive, since the dislocations disappear. It is also highly non-reversible, since both the potential (= elastic) energy and the kinetic energy of the dislocations will be dissipated.

Fig. 4 illustrates the situation when two groups of edge dislocations encounter each other on *neighbouring parallel glide planes*. If the glide planes are sufficiently close together, the dislocations will annihilate pairwise, too, but now leaving behind intrinsic atomic defects. If the 'inserted planes' of the edge dislocations face each other, as in Fig. 4a, these defects will be self-interstitials (or clusters of self-interstitials). If the inserted planes point in opposite directions, the atomic defects generated will be vacancies or vacancy clusters. Analogous arguments hold if the encountering dislocations have mixed character, i.e., if they are neither pure edge nor pure screw dislocations.

The annihilation process of pairs of edge dislocations or of dislocations with large edge components may be looked upon as involving dislocation climb (= dislocation motion perpendicular to their glide planes). Depending on the climb direction, such processes create either self-interstitials or vacancies. Since this type of motion changes the local density of matter in the region through which the dislocations climb, it is termed *non-conservative*. By contrast, glide motions of dislocations preserve the local density of matter; they are therefore called *conservative*.

The preceding considerations apply also to jogs, i.e. the dislocation segments effecting the transition of a dislocation line between two neighbouring glide planes. Since a jog, although its length may be as short as the interatomic distance, is part of a dislocation line with a definite Burgers vector, a glide plane may be ascribed to it. Hence, the distinction between conservative and non-conservative motions applies to jogs as well. The motion of a jog in a screw dislocation is conservative if it occurs along a stationary dislocation line, and non-conservative if the jog is dragged along by the gliding dislocation. For jogs in edge dislocations the opposite is true. In general, the jog motion during plastic deformation consists of sequences of conservative and non-conservative movements.

---

[8] The minimum stress required to achieve permanent ("plastic") deformation is called the *critical shear stress* and usually denoted by σ_0. The above discussion aims at illustrating the various theoretical concepts and is not meant to imply that the critical shear stress of crystals is determined by the stress required to operate Frank–Read sources. On the contrary, crystals appear always to contain such a wide distribution of the distances between the anchoring points of grown-in dislocations that a variety of other obstacles to long-range dislocation motion are more important than the Frank–Read source "lengths", which determine the stress that must act on a dislocation in an otherwise perfect environment for the Frank–Read mechanism to start. In fact, electron, X-ray, or optical micrographs in which one sees unequivocal evidence for this mechanism are still rarities.

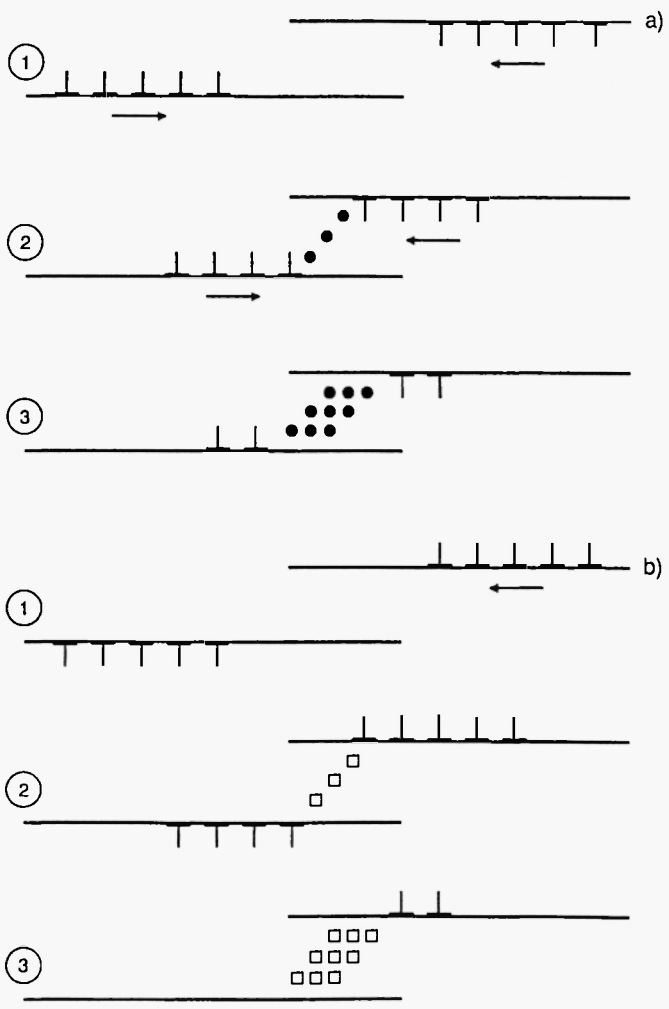

Fig. 4: Formation of interstitial (a) or vacancy (b) clusters by the annihilation of groups of edge dislocations of opposite sign on neigh-bouring glide planes. Full circles indicate self-interstitials, open squares vacancies. The numbering denotes successive stages of the encountering + annihilation processes.

Table 1 summarizes the three dichotomies that have been discussed in this section.

The annihilation of *screw dislocations* of opposite sign by cross-slip referred to above is a conservative process and, by itself, does not create atomic defects. However, since cross-slip invariably occurs only over limited lengths of the dislocations, dislocation segments with large edge components are left behind. These may climb by the absorption or emission of vacancies and interstitials and arrange themselves in energetically favourable patterns of dislocations of the same sign that are similar to small-angle grain boundaries /10/. This is one of the mechanisms by which the

Table 1:
The thermodynamic and kinematic dichotomies of dislocation movement.

Thermodynamics	reversible mechanical work expended during loading is recovered completely during unloading (elastic behaviour)	irreversible mechanical work is partly transformed into heat (in anelasticity to a small degree, in plastic deformation to a large degree)
dislocation (jog) movement (kinematics)	inversive dislocations follow the same paths during loading and unloading	non-inversive dislocations follow different paths during loading and unloading
	conservative no generation of vacancies or interstitial atoms (local density conserved)	non-conservative generation of vacancies and/or interstitial atoms and of vacancy and/ or interstitial clusters

annihilation of dislocations of opposite sign, a strongly dissipative process, may lead to *ordered arrangements of dislocations of the same sign*. Similarly, if groups of dislocations with large edge components of the same sign meet on parallel glide planes, they may reduce their energy by taking up ordered structures by moving non-conservatively.

The self-organization processes described in the preceding paragraph are generalizations of the *Lück–Sizmann effect*. More than 30 years ago, Lück and Sizmann /15/ pointed out that even if vacancies and self-interstitials are generated randomly in radiation-damage experiments, there will be a tendency for them to form clusters of defects of the same sign. The reason for this is that interstitials deposited near vacancies during continuing irradiation (or vacancies created close to pre-existing interstitials) annihilate, whereas atomic defects created close to defects of the same kind tend to "survive" even at high defect densities. This is a self-organization process that may lead to ordered structures observable by transmission electron microscopy /16,17/.

Further generalizations of the Lück–Sizmann effect, associated with the dislocation reactions discussed above as well as with defect clusters, are of great importance in prolonged cyclic deformation. They will be treated in Sect. 4.

3. CYCLIC HARDENING OF FCC METALS

In this section we outline an 'abstract' theory of cyclic hardening, based on a few simple

hypotheses, and discuss its main predictions. Its 'realization' in terms of specific mechanisms will be the subject of Sect. 4.

The basic hypotheses of the theory are as follows:

(*i*) The flow stress of fatigue-hardened fcc metals may be described by the superposition of *two* hardening mechanics, one of which is specific for cyclic deformation.

(*ii*) One of the mechanisms has (essentially) the properties of the Stage-I work-hardening of unidirectional deformation of single crystals orientated for glide on a single glide system /10/. Its contribution to the flow stress, σ_M, is independent of the strain rate $|\dot{\varepsilon}_{pl}|$ and depends only weakly on temperature. This weak T-dependence is considered to be a consequence of the temperature dependence of the elastic moduli; whence the notation σ_M.

(*iii*) To the second hardening mechanism (the one specific for cyclic deformation) the following properties are attributed:

(a) Its contribution to the flow stress is strongly $\dot{\varepsilon}_{pl}$- and T-dependent. The underlying physical picture is that the second hardening mechanism involves *short-range interactions* of the glide dislocations with fairly localized 'obstacles', which may be overcome with the assistance of thermal fluctuations. This contribution to the flow stress will be denoted as *obstacle contribution* σ_{obs}; hence the total flow stress is written as

$$\sigma = \sigma_M + \sigma_{obs} \tag{4}$$

(b) Nucleation and growth of the obstacles referred to in item (a) are self-organization processes.

(c) The dislocation movement during cyclic plastic deformation may *accelerate* the formation and growth of the obstacles as well as *destroy* them or, at least, reduce their strength.

(*iv*) In low-amplitude cyclic deformation the σ_{obs}-contribution to the flow stress builds up gradually after the first half-cycle. (The first half-cycle corresponds, as a matter of course, to deformation in Stage I of the unidirectional work-hardening curve and subsequent unloading – cf. (*ii*).) The fraction σ_{obs}/σ increases monotonically with increasing $\varepsilon_{pl,cum}$ (and increasing σ). Except at and close to saturation, for fixed values of the "external" parameters T, $\hat{\varepsilon}_{pl}$, and $|\dot{\varepsilon}_{pl}|$, there is a unique relationship between σ and σ_{obs}.

(*v*) The two "phases" in regime B of the cyclic stress–strain curve differ in the subdivision of $\hat{\sigma}_{sat}$ into σ_M and σ_{obs}, such that σ_{obs} is larger in the 'high-$\hat{\varepsilon}_{pl}$ phase' than in the 'low-$\hat{\varepsilon}_{pl}$ phase'.

Once the coexistence in mechanical equilibrium of the two phases in regime B of the cyclic stress–strain curve of the saturated state is accepted as an experimental fact, hypothesis (*v*) may be deduced from the other hypotheses by physical reasoning as follows. Since the only 'internal' parameters of the present description are σ_M and σ_{obs}, and since the coexistence of the two phases at the temperature of the cyclic deformation implies that both phases have the same flow stress, they must differ in their

$\sigma_{obs}/\hat{\sigma}_{sat}$ -ratios [9]. During the cyclic hardening, the specimen passed through all σ_{obs}/σ values from zero to $\sigma_{obs}/\hat{\sigma}_{sat}$. In view of the uniqueness of the $\sigma_{obs}=\sigma_{obs}(\sigma)$ relationship (for fixed T, $\hat{\varepsilon}_{pl}$, and $|\dot{\varepsilon}_{pl}|$ during cyclic hardening it would be very hard to imagine a second, radically different state with the same $\sigma_{obs}/\hat{\sigma}_{sat}$ ratio. From this it follows that $\sigma_{obs}/\hat{\sigma}_{sat}$ must indeed be *larger* in the high-$\hat{\varepsilon}_{pl}$ phase than in the low-$\hat{\varepsilon}_{pl}$ phase and, by the arguments of footnote 9, that it must be so by a finite amount.

It will now be shown that the above hypotheses can account for the most salient features of cyclic plastic deformation, in some cases in a non-trivial manner.

(*1*) The dependence of the saturation stress on the temperature of deformation /18, 19/ is much larger than that of the flow stress of uniaxially deformed fcc single crystals. An analogous statement holds for the strain-rate sensitivity of $\hat{\sigma}_{sat}$ /19/. These observations (on Cu single crystals) are accounted for by the obstacle contribution to the flow stress.

(*2*) The cyclic hardening curves as measured at different temperatures show a cross-over phenomenon [18, 19]. Whereas in the saturation regime the temperature dependence is "normal" ($d\hat{\sigma}_{sat}/dT > 0$, $d^2\hat{\sigma}_{sat}/dT^2 > 0$), at intermediate $\varepsilon_{pl,cum}$ the $\hat{\sigma}(\varepsilon_{pl.cum})$-curves measured at intermediate temperatures may lie below those measured at higher temperatures. This would be hard to understand if only one mechanism contributed to the cyclic hardening. It does find a simple explanation if there are two contributions to the flow stress such that the gradual build-up of the one with the stronger temperature dependence (i.e., of σ_{obs}) depends on the temperature at which the cyclic deformation is performed. In terms of the hypotheses listed above what is required in order to account for the observations on Cu is that the build-up of the "obstacles" proceeds faster at higher temperatures at least up to 305 K, the highest temperature investigated in the above-mentioned work /19/.

(*3*) If after reaching the saturation state the cyclic deformation is continued at a lower temperature, the deformation remains essentially confined to the pre-existing PSBs, whereas continuation at a higher temperature leads to the formation of *new* PSBs at the expense of the matrix /18/. This behaviour follows immediately from Fig. 5, in which the temperature dependence of the flow-stress of a crystal cycled to saturation at the temperature T_0 and its subdivision into σ_M and σ_{obs} is shown separately for

---

[9] It might be argued that the system should be described by an additional parameter that is zero in the low-$\hat{\varepsilon}_{pl}$ phase and positive in the high-$\hat{\varepsilon}_{pl}$ phase in such a way that it starts out from zero when saturation begins. Such a parameter would behave like a scalar order parameter in a *second-order phase transition* in the Ehrenfest nomenclature or in a *critical phase transition* in the modern terminology. However, this would not explain the regime B of Fig. 2 with the coexistence of both "phases" in equilibrium, which requires the "phase transition" to be of first order. By the same argument we may exclude the possibility that the high-$\hat{\varepsilon}_{pl}$ phase starts out with the same σ_{obs}/σ-ratio as the low-$\hat{\varepsilon}_{pl}$ phase when it begins to appear upon reaching saturation, since in the critical region σ_{obs}/σ would behave like an order parameter in a second-order phase transition, again in conflict with the observations.

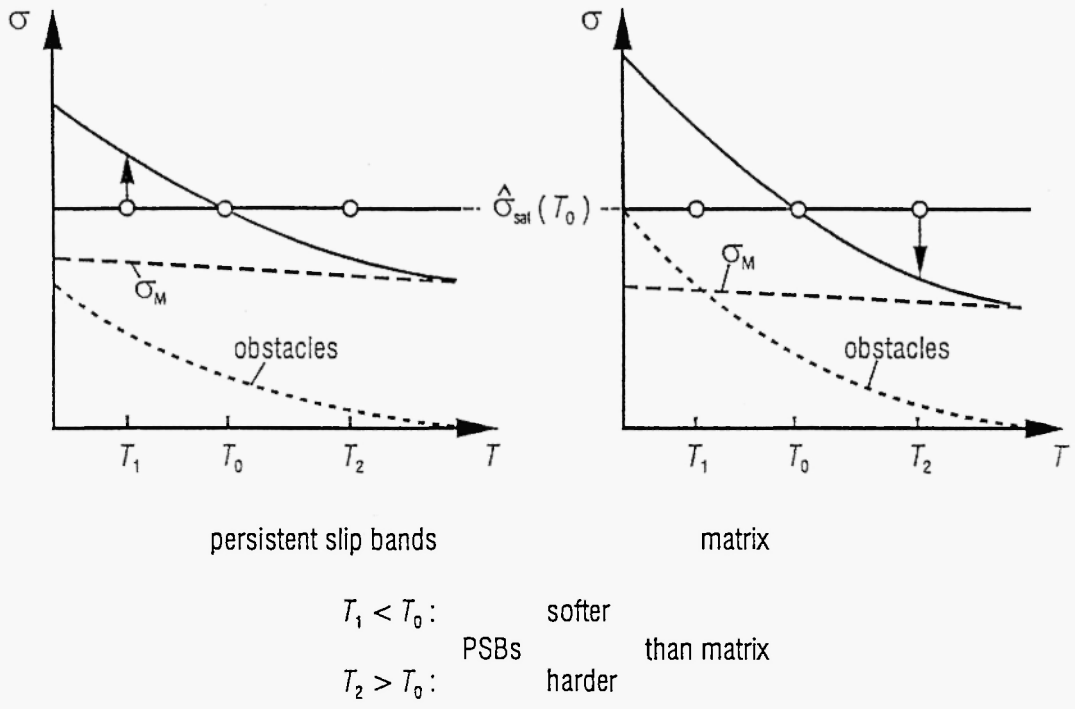

Fig. 5: Temperature dependence of flow stress after cyclic deformation to saturation at temperature T_0, with different subdivisions into the long-range stress σ_M (interrupted line) and the obstacle contribution σ_{obs} (dotted line) in the persistent slip bands and in the matrix.

the PSBs and the matrix. The argument runs as follows. As explained above, the "equilibrium coexistence" of matrix and PSBs implies that at T_0 the flow stress is the same in both phases, namely equal to $\hat{\sigma}_{sat}(T_0)$. The different subdivisions of the flow stress into σ_M and σ_{obs} have the consequence that at temperatures below T_0 the flow stress in the PSBs is lower than that in the matrix, whereas the reverse is true if the temperature is raised above T_0 (cf. Fig. 5). Therefore, after lowering the temperature, the deformation is expected to be concentrated entirely in the pre-existing PSBs. If, however, the temperature is raised above T_0, the matrix is softer than the PSBs, so that now the contribution of the matrix to the average strain is larger than it was at T_0. This will result in the formation of additional slip bands or the extension of the pre-existing ones at the expense of the matrix.

The perpendicular arrows in Fig. 5 indicate the instantaneous changes of the flow stress when the temperature of deformation is lowered or increased. From the above discussion it follows that changes to lower temperatures or higher strain rates allow us to study the temperature and strain-rate dependence of the flow stress in the slip bands (see, e.g., /19/). Under changes to higher temperatures or lower strain rates, however, the microstructure in the saturation regime is unstable against the

transformation "matrix ⇒ PSBs" (cf. Table 2). This has the consequence that studies of the flow stress in the *matrix* by change-in-temperature or change-in-strain-rate test must be performed either well *before* saturation or in the regime A of the cyclic stress–strain curve.

Table 2:

Effects of changes of temperature or plastic strain-rate on the microstructure of cyclically deformed crystals with matrix and persistent slip bands coexisting (regime B of the cyclic stress–strain curve.

lowering *increasing*

the temperature of deformation, and/or

increasing *decreasing*

the plastic strain-rate $|\dot{\varepsilon}_{pl}|$

makes the persistent slip bands

softer *harder*

than the matrix. The further deformation will therefore tend to take place in the

slip bands *matrix.*

Thus the microstructure of fatigued crystals with coexisting matrix and PSBs is

stable

if the temperature is lowered or $|\dot{\varepsilon}_{pl}|$ is increased, but

unstable

if the temperature is raised or $|\dot{\varepsilon}_{pl}|$ is decreased.

4. SELF-ORGANIZATION PROCESSES AND THE INTERACTION BETWEEN DISLOCATIONS AND INTRINSIC ATOMIC DEFECTS

In this section it will be shown that a model satisfying the hypotheses (*i*)-(*v*) of Sect. 3 may be developed on the basis of the known properties of dislocations and atomic defects and of the general considerations of Sect. 2.

Let us first consider a dislocation line containing well-separated short jogs of opposite sign. In Fig. 6 the jogs are marked by circles with + or – signs, the + signs corresponding to vacancy

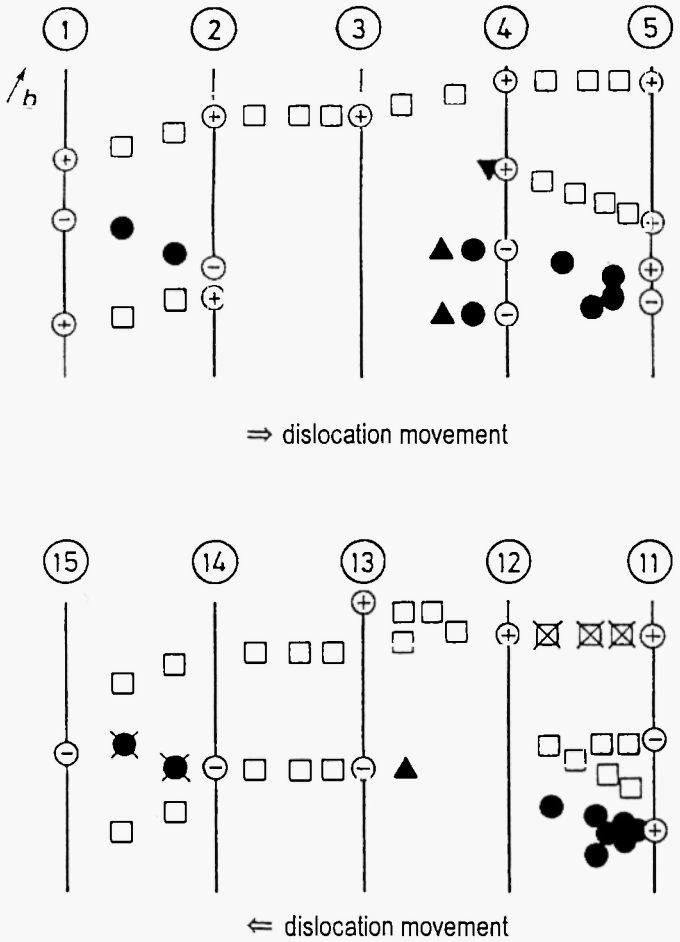

Fig. 6: Generation of vacancies and self-interstitials (both isolated and as clusters) by the movement of jogs in dislocations.

production when the jogs perform non-conservative movements from left to right. The successive positions of the dislocation line in its glide plane as well as the location of its jogs during its movement from left to right are indicated by the numbering 1-5. Jogs on the same dislocation line but of opposite sign will annihilate when they encounter each other. (In the example of Fig. 6, this has occurred between positions 2 and 3.) The movement of jogs perpendicular to the Burgers vector $\boldsymbol{b}$ of the dislocation creates vacancies (open squares) or self-interstitials (full circles), depending on the sign and direction of motion of the jogs. If a jog moves approximately perpendicularly to $\boldsymbol{b}$ over several interatomic distances (this may happen for jogs in screw dislocations), *rows* of atomic defects are created. An example of this is shown between positions 4 and 5.

During its glide movement a dislocation may intersect dislocations threading its glide plane. In Fig. 6 locations of such dislocations are marked by full triangles. Each intersection process generates a jog in the gliding dislocation unless the Burgers vector of the threading dislocation happens to lie in the glide plane of the moving dislocations. In Fig. 6 such intersection processes had taken place just before position 4 was reached. The sign of the jogs created depends on the sign of the scalar product of the Burgers vector and the glide-plane normal of the intersected dislocations.

The lower half of Fig. 6 illustrates what may occur when, after reversing the force acting on it, a dislocation passes once more over the same area it had swept out before. Jogs that produced vacancies during the motion from left to right will now produce interstitials. If during unloading the jogs follow approximately the same paths as during the loading (in the nomenclature of Sect. 2: if their motion is approximately *inversive*) the atomic defects created during the return movement will annihilate those created during the first passage. (In Fig. 6 annihilation of atomic defects is indicated by crosses.) Since the energy that had been stored in the atomic defects will be dissipated as heat, this is an example of an *inversive* dislocation motion that is strongly *irreversible* even in the absence of frictional forces or potential barriers. On the other hand, it may happen that a + jog creates defects in an area in which during the opposite motion a – jog has left behind defects of the same sign. This will contribute to the formation of *defect clusters*. If in cyclic deformation many dislocations carrying jogs pass through a certain area, the processes just described will produce spatially separated clusters of vacancies and interstitials, in close analogy to the Lück–Sizmann effect in radiation damage experiments. Therefore, it appears justified to refer to these processes as resulting from a generalized Lück–Sizmann effect (cf. Sect. 2).

So far, there has been no reference to the temperature of deformation. As they stand, the preceding considerations apply to sufficiently low temperatures. Since the energy stored in the atomic defects is supplied almost entirely by the external load and *not* by temperature fluctuations, in the temperature range with a pronounced regime B of the cyclic stress–strain curve and therefore little cross-slip, temperature plays only a minor rôle in the *defect production*. However, there is a very strong influence of the temperature of deformation through the temperature dependence of the *mobility* of the atomic defects, which increases rapidly with increasing temperature. Because of this, at high

temperatures the defect clusters will be more compact than at low temperatures and may even be converted into dislocation loops or stacking-fault tetrahedra [10]. Above the so-called Stage-III temperature [11] isolated self-interstitials are no longer present; they will either have annihilated instantaneously with vacancies or will have formed clusters together with other interstitials. In the fcc metals, divacancies (= pairs of vacant neighbour sites) generated by the cyclic deformation will anneal out instantaneously at about the same temperature as the self-interstitials. Isolated vacancies will disappear during deformation at somewhat higher temperatures either by joining vacancy clusters or by being absorbed by interstitial clusters or dislocations.

We identify the "obstacles" of Sect. 2 with the vacancy and interstitial clusters. Their efficiency as obstacles to the dislocation motion depends on their size, compactness, and nature (vacancy or interstitial type). E.g., isolated atomic defects and very small clusters impede the dislocation motion only at very low temperatures. Therefore, the disappearance of isolated interstitials and small interstitial clusters at intermediate temperatures does not directly affect the flow stress at these temperatures whereas the increase in size and compactness of the clusters does. Analogous arguments hold for vacancy clusters formed by the agglomeration processes described above as well as for the clusters generated by the annihilation of dislocations of opposite sign to be discussed presently.

---

[10] At temperatures high enough for major rearrangements within the clusters to occur, interstitials and vacancies behave very differently. According to the evidence from transmission electron microscopy in fcc metals, self-interstitials tend to form dislocation loops of the Frank type (i.e., their Burgers vectors do *not* lie in the planes of the loops). They may or may not contain a stacking fault. Vacancies may form voids, stacking-fault tetrahedra, or Frank-type dislocation loops. For energetic reasons, the first two tend to prevail as long as the number of vacancies per cluster is small; large clusters will form loops, as in the case of interstitials. An apparent exception to this rule of thumb occurs when the voids are stabilized by gaseous impurities. Such "bubbles" may grow very large. Near-surface bubbles are presumably responsible for the formation of fatigue cracks. It is indeed a long-established experimental fact that the fatigue life depends strongly on the atmosphere in which the fatigue tests are performed. – Since in the present paper the questions of crack formation and fatigue life are not treated, we shall continue to speak of "defect clusters" without regard to their configurations.

[11] This nomenclature is not to be confused with the stages of the unidirectional work-hardening curve /10/. It refers to the recovery of the residual electrical resistivity of metals after low-temperature irradiation with energetic particle (so-called radiation damage), which in isochronal annealing experiments (fixed annealing times at successively higher temperatures) recovers in fairly well-defined "stages" at characteristic temperatures (see, e.g., [20] and the Appendix). – In typical isochronal annealing experiments [annealing time $(0.5–2) \cdot 10^3$ s] Stage III is observed in Cu between 210 K and 240 K, depending on the concentration of atomic defects involved. However, since typical cyclic deformation experiments last about a factor of 10 longer than typical annealing experiments and since the defect concentrations in the saturation regime are very high, the temperatures of the recovery stage III are shifted to lower temperatures compared with typical electron-irradiation studies. In typical cyclic–deformation experiments on Cu we may expect the Stage-III temperature to lie between 205 K and 215 K. These matters will be taken up in the Appendix in a discussion of the electrical resistivity work of Basinski and Basinski /21/.

As discussed in Sect. 2, when two dislocations of opposite sign annihilate, a large number of atomic defects may be created, the more the closer the character of the annihilating dislocations is to edge dislocations. Two edge dislocations annihilating gradually by climb leave behind a platelet of interstitials or vacancies. Annihilating dislocations of mixed character generate looser clusters which, however, at elevated temperatures may become compact by diffusion. If the annihilating dislocations are members of two trains of dislocations sent out by Frank-Read sources located on neighbouring glide planes, the processes just described will be repeated every time two dislocations meet, so that quite large clusters may result from their annihilation.

In addition to the mechanisms so far discussed there is the "normal" hardening due to the long-range stresses of the dislocations. Averaged over the entire sample, the stresses originating from the dislocations are, of course, zero. The *flow stress* is determined by those obstacles which are located where the long-range internal stresses are large and opposite to the applied stress. This means that the present model meets the requirements of the hypotheses (*i*) and (*ii*) of Sect. 3.

It is easy to see that the model is in accord with the requirements of items (a) and (b) of hypothesis (*iii*) and of hypothesis (*iv*), too. Item (*v*) has already been dealt with in Sect. 3. The remaining item (*iii*, c), which in the present writer's opinion is crucial for the understanding of cyclic deformation but has so far found insufficient attention in the literature, will be discussed in the next paragraph.

At temperatures and stresses at which neither cross-slip nor climb of isolated dislocations is significant (in contrast to the climb of close pairs of dislocations of opposite sign, so-called dislocation dipoles), the only alternatives for mobile dislocations encountering a cluster obstacle are to get stuck at it until the stress direction is reversed or to cut through it. The second possibility is illustrated in Fig. 7. For the sake of the argument it is assumed that a group of edge dislocations on the same glide plane has cut a large cluster into two halves and has shifted them with respect to each other by the total Burgers vector of the dislocation group. What happens when the load is reversed depends critically on whether the dislocation motion between the cutting and the return was inversive or non-inversive. In the first case (top half of Fig. 7) the cut cluster is restored; hence the cutting was without any permanent effect other than the dissipation of energy. The second case is illustrated in the bottom half of Fig. 7. Here it is assumed that after having bisected the cluster, the dislocation group annihilates with a group of opposite sign, giving rise to a new cluster. Since now there are no dislocations that might return following the loading path, the first cluster stays bisected. Its two halves may be too small to have a significant effect on the flow stress or – if the temperature is high enough – disperse altogether. We thus see that the proposed model meets the requirements of item (*iii*, c), too.

A further important feature of the cutting-and-shifting mechanism results from the fact that the large-amplitude cyclic dislocation motion, as it occurs in the PSBs, causes the cluster segments to be shifted around slowly but quite significantly. If in this process a segment happens to meet one of the opposite sign, it annihilates partially or even totally, which means that it becomes smaller or even vanishes. On the other hand, if a cluster segment encounters a cluster of the same sign, a larger cluster will result. Thus we see that, in a further kind of a generalized Lück-Sizmann effect, the

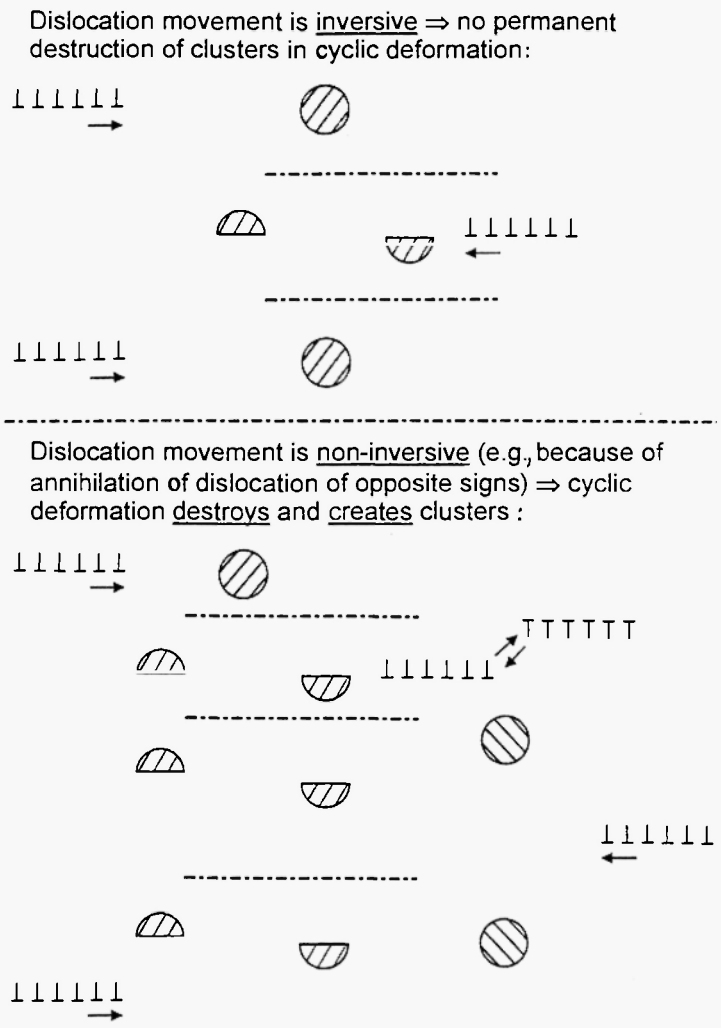

Fig. 7: Cutting of obstacles (hatched circles) by groups of dislocations. Top: The inversive return motion of the dislocations restores the obstacles. Bottom: After cutting the obstacles, the dislocations annihilate with dislocations of opposite sign. The return motion does not restore the original obstacles. The dislocation annihilation has generated new obstacles (indicated by different hatching).

large-amplitude to-and-fro motion of the dislocations in the PSBs contributes to the coarsening of the cluster distributions.

The remainder of the section will be devoted to a discussion of the saturation of the flow stress, of the origin of the instability that leads to PSB formation, and of the mechanisms that determine ε_{PSB}, the strain amplitude in the PSBs.

The *saturation* of the cyclic hardening curve clearly indicates that the fatigued specimen has now

reached a state of quasi-equilibrium, in which no further hardening occurs. The quasi-equilibrium must be a *dynamic* one, as may be seen from the fact that in this state the energy dissipation is very high indeed. Since the σ–ε loops in the saturation regime are almost rectangular, the energy dissipated per cycle and unit volume, w_ε, is only slightly less than $4\hat{\varepsilon}_{pl}\hat{\sigma}_{sat}$. From the experiments on Cu crystals by Basinski and Basinski /19/ at 4.2 K we obtain the estimate

$$w_\varepsilon \approx 4 \cdot 2 \cdot 10^{-3} \cdot 85 \cdot 10^6 \text{ J/m}^3 = 6.8 \cdot 10^5 \text{ J/m}^3, \tag{5a}$$

whereas at room temperature the corresponding quantity is

$$w_\varepsilon \approx 4 \cdot 2 \cdot 10^{-3} \cdot 28 \cdot 10^6 \text{ J/m}^3 = 2.2 \cdot 10^5 \text{ J/m}^3. \tag{5b}$$

These are quite large values, indicating that the annihilation of dislocations of opposite sign is a major if not the main contributor to the energy dissipation /7/.

In the saturation state we have presumably not only dynamic equilibrium between the multiplication and the annihilation of dislocations but also distributions of the obstacle sizes that approach states of dynamic equilibrium. Since this involves the rather slow shifting around of the cluster segments discussed above, the approach to the quasi-equilibrium distributions of defect clusters is expected to take much longer than the establishing of the dynamic equilibrium of the dislocations. This expectation is supported by the following two observations of Basinski and Basinski /19/. (*1*) For Cu crystals cycled with $\hat{\varepsilon}_{pl} = 2 \cdot 10^{-3}$ at various temperatures between 230 K and 305 K a cumulative strain of 10 to 20 suffices to reach saturation, whereas at 4.2 K saturation sets in only at $\varepsilon_{pl,cum} \sim 10^2$. Since the fairly strong monotonic temperature dependence of the flow stress characteristic of $\hat{\sigma}_{sat}$ (cf. Sect. 3) develops only at $\hat{\varepsilon}_{pl,cum} \geq 10$ and since this temperature dependence is attributed to the presence of a wide distribution of obstacle strengths, we may conclude that to achieve dynamic quasi-equilibrium takes indeed much longer for the cluster distribution than for the dislocations. (*2*) At temperatures from 60 K upwards the cyclic hardening curve "overshoots" before $\hat{\sigma}_{sat}$ is reached; i.e., there is a regime with $\sigma > \hat{\sigma}_{sat}$. This can be understood if during the build-up of the obstacles an intermediate distribution develops that gives a larger $\hat{\sigma}_{obs}$ contribution than the final distribution, whose establishment takes longer than that of the quasi-equilibrium distribution of the dislocations. Both observations just mentioned fit into the present model since, even when the dislocation distribution has become stationary on the scale of many cycles, the generalized Lück–Sizmann effect resulting from the cutting and shifting of the obstacles may continue for a large number of cycles.

It is now relatively easy to understand the *formation of persistent slip bands*. According to the deductions of the preceding paragraphs, in the final stage of the approach to saturation it is mainly the σ_{obs} contribution that is responsible for the increase of the flow stress with increasing $\varepsilon_{pl,cum}$.

However, if $\hat{\varepsilon}_{pl}$ and therefore the amplitude of the dislocation motion is sufficiently large, the peak stress, increasing with σ_{obs}/σ, may become large enough for the dislocations to cut through a sufficiently large number of neighbouring obstacles to allow them to suddenly move over substantially larger distances than before. About half of these dislocations will encounter dislocations of the opposite sign and annihilate them before they are held up again. Because of the dislocation annihilation, such a limited "breakthrough" may locally reduce σ_M. If this happens, at peak stress there will be an increase of the "pressure" on adjacent obstacles that up to then were still capable of holding up dislocations. The yielding of some of these obstacles will lead to an avalanche-type breakdown. By a percolation process these avalanches may combine to destroy the matrix microstructure over macroscopic distances. We believe that the persistent slip bands develop along such percolation paths.

As discussed above, in the persistent slip bands the subdivision of $\hat{\sigma}_{sat}$ into σ_M and σ_{obs} is different from that in the matrix, σ_{obs} being larger and σ_M being smaller than in the matrix. The direction of these changes is a consequence of the breakdown mechanism just described. In the first stage of the breakdown the dislocation density, responsible for σ_M, is reduced by the annihilation processes. Dislocation movements with much larger amplitudes than in the matrix become possible. This results in drastically increased rates of production of atomic defects and defect clusters as well as in an enhancement of the generalized Lück–Sizmann effect discussed above. In agreement with the observations /3, 5/, the change-over from the microstructure of the matrix to that of the PSBs is therefore predicted to proceed within quite a small number of cycles.

The fact that under given external conditions the *strain amplitudes in the persistent slip bands*, ε_{PSB}, assume fairly well defined values can be understood as the outcome of a balance between the work-hardening associated with the build-up of long-range stresses and the destruction of obstacles by the dislocation movement. If the strain amplitude is less than ε_{PSB}, the destruction of obstacles required for the PSB formation is too slow to reach a quasi-stationary state. On the other hand, if the strain amplitude is higher than ε_{PSB}, additional hardening takes place due to increasing long-range stresses. In either case, balance with the $\hat{\sigma}_{sat}$ value prescribed by the matrix microstructure cannot be achieved, hence the strain amplitude "settles" for a definite value that gives the same flow stress in the PSBs as in the matrix.

Seeger and Frank /7/ have shown that the macroscopic data on regime B of the cyclic stress-strain curve can be reconciled with the electron-microscopy observations on dislocation densities etc. in the PSBs only if the lifetime of a dislocation segment in a PSB is distinctly shorter than the cycling period. This means that in the persistent slip bands there must be a strong activity in dislocation multiplication and annihilation during each cycle. Transmission electron microscopy shows that the dislocations participating in these processes have predominantly screw character. Hence they annihilate with little atomic-defect generation. This led Seeger and Frank /7/ to suggest that an approximate relationship between ε_{PSB} and $\hat{\sigma}_{sat}$ might be derived by considering the dislocation

processes only. In this way they obtained the relationship

$$\hat{\varepsilon}_{PSB} = \frac{n_{ann}}{n} \cdot \frac{1}{8\alpha^2 M_s} \hat{\sigma}^{M}_{sat} \quad , \tag{6}$$

where n_{ann}/n (<< 1) denotes the ratio of two dislocation densities, namely that of the dislocations annihilating during one cycle and that of the screw dislocations in the PSBs. The parameter α characterizes the σ_M-contribution to the saturation stress according to

$$\hat{\sigma}^{M}_{sat} = aM_s bn^{1/2} \quad . \tag{7}$$

In (7), M_s is the relevant shear modulus (for screw dislocations in an elastically isotropic medium given by the shear modulus) and b the dislocation strength. With n_{ann}/n values compatible with the electron microscopy observations and the plausible value α = 0.3, Eq. (6) accounts for $\hat{\varepsilon}_{PSB}$ and $\hat{\sigma}_{sat}$ in Cu at room temperature, where $\hat{\sigma}^{M}_{sat}$ is presumably not much less than $\hat{\sigma}_{sat}$ /3,7/. In the case of Cu, Eq. (6) might be tested by measurements above room temperature although, of course, it will fail as the "critical temperature" of the two-phase model will be approached, since there $\hat{\varepsilon}_{PSB}$ goes to zero whereas $\hat{\sigma}_{sat}$ does not.

5. CONCLUSIONS

The theory [12] of hardening by cyclic plastic deformation and of the formation at persistent slip bands (PSBs) presented in the present paper explains the persistent slip bands observed in face-centred cubic metals and other crystal structures (but not in body-centred cubic metals) as *long-lived* (thermodynamically metastable) quasistationary *dissipative structures*. According to the theory, PSBs are formed by *coupled* self-organization processes of dislocations and intrinsic atomic defects (lattice vacancies and self-interstitials). The main mechanism of the *dislocation self-organization* is the *annihilation* of dislocations of *opposite* sign and the *accumulation* of dislocations of the *same* sign with predominant edge character. The self-organization of the *atomic defects* comes about by the annihilation of vacancies and self-interstitials that are generated as neighbours. By the so-called Lück–Sizmann effect, well established in radiation damage studies, this leads to an *agglomeration* of defects of the same sign, i.e. to the formation of interstitial and vacancy clusters.

[12] Here "theory" is meant in the original greek meaning of θεωρια, viz. "a looking at, viewing, contemplation" /22/.

The *coupling* between the self-organization processes of dislocations and those of intrinsic atomic defects is effected predominantly by two mechanisms: (*i*) The generation of atomic defects (isolated or clustered) by the non-conservative movements of jogs in dislocations and the annihilation of dislocations of non-screw character. (*ii*) The cutting and dispersing of the clusters of atomic defects by the cyclic motion of the dislocations, which, however, has to be *non-inversive*. The shifting around of the cluster segments brought about by this leads to a *generalized Lück–Sizmann effect*: Clusters or cluster segments of the opposite sign that encounter each other annihilate partially or totally, whereas the meeting of clusters of the same sign will result in larger clusters. In this way a quasi-stationary distribution of defect clusters of different sizes is built up during the cyclic deformation. The clusters act as obstacles to the dislocation motion. Unless they can be circumvented by cross-slip (in materials such as Cu with intermediate stacking-fault energies this happens only at elevated temperatures and stresses), the dislocations get either stuck at the larger obstacles or cut through them under the combined action of stress and temperature. At sufficiently large plastic strain amplitudes, the destruction of the obstacles by the moving dislocations gives rise to an instability of the obstacle–dislocation pattern built up during the early cycles of fatigue tests. By a percolation process, this instability leads to the formation of persistent slip bands (PSBs), in agreement with the two-phase picture of Winter.

The coupled self-organization mechanisms account well for the main features of both the cyclic-hardening curve and the cyclic stress-strain curve of face-centred cubic metals, including such details as the temperature dependence of the flow stress, the influence of the temperature of deformation, the absence of persisted slip-bands in high-temperature fatigue, and the stability/ instability of the matrix–PSBs microstructure of fatigued metals when the cyclic deformation is continued at lower/higher temperatures.

APPENDIX
ELECTRICAL RESISTIVITY STUDIES OF FATIGUE IN METALS

In footnote 11 brief reference has been made to the study of the cyclic deformation of metals by means of measurements of the residual electrical resistance. The residual electrical resistivity of metals is very sensitive against the presence of atomic defects, the physical reasons for this being, on the one hand, that even in a non-superconducting defect-free metal the electrical resistivity goes to zero as the absolute zero of temperature is approached and, on the other hand, that the disturbance of the perfect crystal structure by atomic defects extends at most over a few wavelengths of the electrons at the Fermi surfaces. Atomic defects, therefore, scatter these electrons very efficiently and dominate, in the form of impurities, the low-temperature resistivity even of 'pure' metals. The decrease of the ratio of the electron wavelengths to the extension of the scattering potential with increasing cluster size causes the resistivity per vacancy or self-interstitial to decrease as larger and larger clusters are

formed by the Lück–Sizmann mechanism discussed in Sect. 4. Resistivity measurements are thus complementary to measurements of the flow stress, whose temperature dependence is predominantly determined by the *large* defect clusters.

It is surprising that relatively little use has been made of electrical-resistance measurements as a tool for studying the role of intrinsic atomic defects in the low-amplitude cyclic deformation of metals. The following discussion will be based on the work of Basinski and Basinski /21/ on Cu single crystals fatigued at low temperatures. These authors correlated their resistivity measurements particularly well with the mechanical and microstructural properties. Since, as will be seen, some of their results are significant beyond the field of cyclic deformation, we discuss them separately from the main body of the paper. As a fringe benefit, this separation makes it evident that the line of reasoning in the main text does not depend on the resistivity data and that, therefore, their discussion in terms of the mechanisms of Sect. 4 provides, to some degree, an independent test of the model developed in the present paper.

Fig. A1 shows both the *peak stress*, $\hat{\sigma}$, and the *deformation-induced residual resistivity*, $\Delta\rho$, of a Cu single crystal as a function of the number N of deformation cycles at 14 K. The strain amplitude was $\hat{\varepsilon}_{pl} = 2 \cdot 10^{-3}$, hence according to the definition (1) $N = 5 \cdot 10^4$ corresponds to $\varepsilon_{pl,cum} = 4 \cdot 10^2$. Several features of Fig. A1 are worth noting.

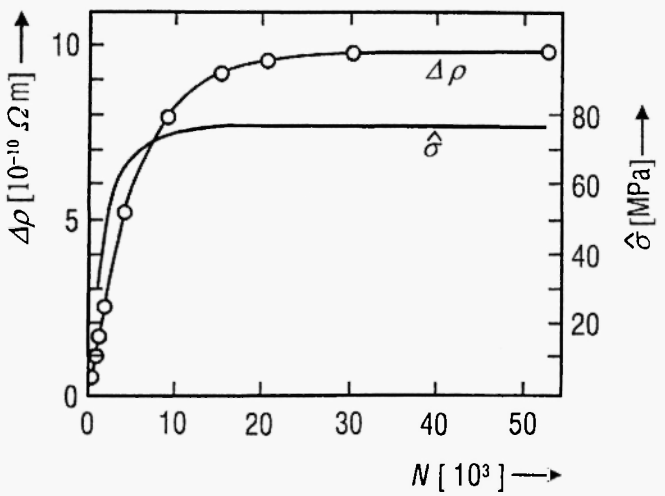

Fig. A1: Peak stress, $\hat{\sigma}$, and change of the residual electrical resistivity, $\Delta\rho$, of a Cu single crystal fatigued at 14 K at $\hat{\varepsilon}_{pl} = 2 \cdot 10^{-3}$ as functions of the number of cycles, N /21/. From $\sigma(N)$ the cyclic-hardening curve $\sigma = \sigma(\varepsilon_{pl.cum})$ is obtained by making use of $\varepsilon_{pl.cum} = 4N\hat{\varepsilon}_{pl}$.

(*1*) The saturation resistivity $\Delta\rho_{sat} = 1 \cdot 10^{-9}$ Ωm is rather high. If we assume, for the sake of the argument, that the electrical resistivity per unit atomic concentration of Frenkel pairs is $2.5 \cdot 10^{-6}$ Ωm

and that the entire resistivity change was due to isolated vacancies and self-interstitials, we arrive at a total concentration of atomic defects (vacancies plus self-interstitials) of about $8 \cdot 10^{-4}$. Owing to the considerable clustering that must have taken place at concentrations of this order of magnitude, the true concentration of vacant lattice sites and interstitials is presumably substantially larger, even if we allow for the fact that the scattering of conduction electrons by dislocations also contributes to $\Delta\rho$. (The annealing experiments to be discussed in item (*4*) demonstrate that the main contribution does *not* come from dislocations.) [13]

(*2*) The peak stress saturates at a cumulative plastic strain that is lower by a factor 2.5 to 3 (depending on the definition of saturation) than that required to saturate $\Delta\rho$. As discussed in Sect. 4, on the stress level of $\hat{\sigma}_{sat}$ the flow stress is insensitive against both isolated atomic defects and very small defect agglomerates (divacancies, di-interstitials, ...). On the other hand, the contribution per vacancy or per interstitial to the electrical resistivity is largest for isolated defects. We therefore have to conclude that even when the densities of dislocations and large defect clusters have become stationary, the net production of intrinsic atomic defects continues. (Coarsening of the size distribution of small defect clusters by a generalized Lück–Sizmann effect without generation of additional defects would cause $\Delta\rho$ to *decrease* with increasing $\varepsilon_{pl,cum}$.) This means that the to-and-fro motion of the dislocations in the saturation regime must be ***non-inversive*** (cf. Sect. 2). Since the mobile dislocations in the PSBs have predominantly screw character, it is presumably their annihilation by cross-slip that brings about the required non-inversiveness of the dislocation motion. This conclusion is in agreement with that of Seeger and Frank /7/, who, on the basis of quite different experimental evidence, argued that in the persistent slip bands dislocation annihilation must be very frequent (cf. Sect. 4). This produces isolated vacancies and interstitials if there are small deviations from the screw character of annihilating dislocations or if jogs are dragged along by the screw dislocations. Since at the temperature of deformation (14 K) the atomic defects do not move by individual jumps, the saturation of $\Delta\rho$ should indeed be reached at much higher $\varepsilon_{pl,cum}$ than that of $\hat{\sigma}$.

(*3*) The ratio of the initial values of $d\hat{\sigma}/dN$ and $d\Delta\rho/dN$ is only one half of $\sigma_{sat}/\Delta\rho_{sat}$. This is in agreement with the concept that with increasing $\varepsilon_{pl,cum}$ the generalized Lück–Sizmann effect causes more and more isolated atomic defects to accumulate in larger clusters and thus reduces their contribution to the resistivity per defect.

---

[13] A quantitative treatment of the electrical resistivity should take into account that, in contrast to the flow stress in the saturation regime, the resistivities in the matrix and in the PSBs differ. The resistivity is expected to be higher in the PSBs, since there the dislocation movement and therefore the rate of generation of intrinsic atomic defects is larger. Since in the measuring geometry the resistances of the matrix and PSBs are "in series", for qualitative discussions of the resistivity in the regimes B and C of the cyclic stress-strain curves it suffices to consider the PSBs. Measurements of the resistivity in the saturation regime as a function of f_{PSB}, which would allow the contributions of the matrix and the PSBs to be determined separately, have apparently not yet been performed but would be informative.

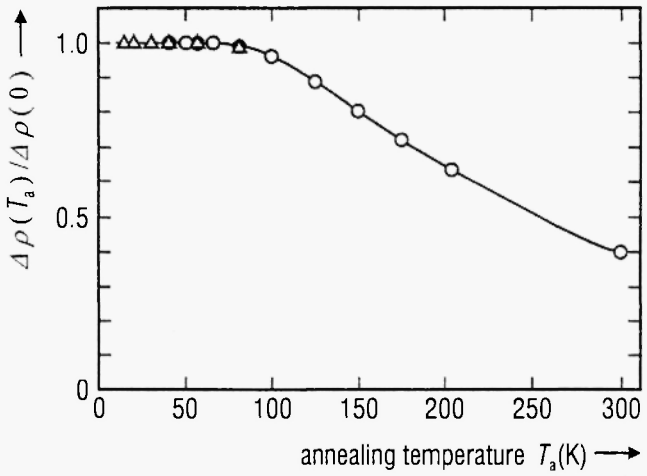

Fig. A2: Recovery of the residual electrical resistivity after low-temperature fatigue of two Cu single crystals (isochronal anneals for $1.8 \cdot 10^3$ s at T_a) [21].$\Delta\rho$ (0) – residual resistivity change due to cyclic deformation at 18 K for $5.5 \cdot 10^4$ cycles (Δ) and at 14 K for $5.25 \cdot 10^4$ cycles (O).

Fig. A2 shows the *recovery* of the residual electrical resistivity of two copper single crystals that had been cyclically deformed with $\hat{\varepsilon}_{pl} = 2 \cdot 10^{-3}$ at 14 K ($\varepsilon_{pl,cum} = 420$) or 18 K ($\varepsilon_{pl,cum} = 440$). At each of the temperatures indicated the samples were annealed for $1.8 \cdot 10^3$ s. Where the two measurements overlap, the recovery curves normalized to the $\Delta\rho$-value after deformation agree with each other, as was to be expected since at the deformation temperature the defect generation is essentially athermal (cf. Sect. 4) and the diffusivity of the defects is negligibly small. Features of Fig. A2 that invite special comment are the following.

(*4*) About 0.6 of the original resistivity had recovered after the 300 K anneal. We can be fairly confident that the dislocation density was not reduced appreciably by the annealing treatment. Therefore, the recovered fraction of the resistivity must have been due to atomic defects and their small clusters. It is indeed well established that in Cu isolated *self-interstitials* and *divacancies* are quite mobile at 300 K. Their disappearance (together with their partners in annihilation reactions) is thought to be responsible for the recovery between 200 K and 300 K. [For the recovery at lower annealing temperatures see item (*5*).] *Monovacancies* diffuse only very sluggishly in Cu at 300 K; a fraction of them will nevertheless have annealed out at 300 K because they provided sinks for the migrating interstitials. The remaining monovacancies would presumably have annealed out if the annealing temperature had been raised to, say, 400 K. The same may be true for some of the small defect clusters. All circumstances considered, we may conclude that only a small fraction of $\Delta\rho_{sat}$, possibly as little as 0.1 or even less, is due to dislocations.

(*5*) The recovery of the electrical resistivity begins only at about 100 K. This is noteworthy in view of the existence of a school of thought /23/ claiming that the self-interstitial configuration of lowest

energy, which in fcc metals is generally accepted to be the so-called <100> dumbbell, migrates in metals such as Cu and Al at about 50 K. There is very strong evidence against this view (see, e.g., /24, 25, 26/), one of the oldest and strongest being that after plastic deformation of fcc metals at liquid-He or liquid-H_2 temperatures the electrical resistivity does not show signs of recovery up to annealing temperatures well above those at which the self-interstitials should have migrated and annealed out (cf., e.g. /20/). The seminal work was that of T.H.Blewitt and his associates on Cu single crystals deformed in tension at 4.2 K /27/. Their observation that there was no resistivity recovery after annealing at 77 K was subsequently confirmed by other authors. Analogous results were found on all other fcc metals investigated [14].

The considerations of Sects. 2 and 4 leave little doubt that the low-temperature cyclic deformation of the crystals investigated by Basinski and Basinski /21/ produced large concentrations of vacancies and self-interstitials and that at the beginning of the annealing treatments enough of the latter were present to have given rise to a detectable recovery below 60 K if they were capable of migrating freely at low temperatures. The fact that Fig. A2 shows no recovery up to about 100 K is thus very convincing evidence that the self-interstitials produced in Cu by plastic deformation do *not* migrate at temperatures of about 50 K. The explanation of the absence of any low-temperature recovery in plastically deformed Cu, Al, Ni etc. is that the self-interstitials seen in radiation-damage experiments to migrate at low temperatures are not in their "ground states" (in which they are if generated during plastic deformation) but in a *metastable* state of higher energy in which they may be created by special processes characteristic of radiation damage [15] [26]. The stable <110>-dumbbell configuration migrates in the recovery stage III referred to in footnote 11, in agreement with the strong recovery seen in Fig. A2 between 200 K and 300 K. This recovery is primarily due to the diffusion of self-interstitials and divacancies to randomly distributed defects or defect clusters of opposite sign. If the reaction partners happen to be close together as, e.g., in a close Frenkel pair, the recovery temperature is lowered partly because now only few migrational steps are needed till annihilation takes place, partly because the energy barrier to migration is lowered. This is thought to account for the recovery between 100 K and 200 K.

In summary, the following may be stated.

(*i*) Information on the mechanisms of cyclic deformation of metals that is complementary to that

---

[14] For references as well as for a discussion of the generation of vacancies and self-interstitials by plastic deformation that goes beyond that of Sect. 2 see /25/.

[15] Because for metals such as Cu, Al, Ni, Ag it postulates the existence of two distinct self-interstitial configurations, the model described above is known as the "two-interstitial model". This name is somewhat misleading, since in at least one fcc metal, viz. Au, in spite of large efforts the low-temperature recovery attributed by the "one-interstitial model" to self-interstitial migration has never been found in radiation damage experiments, let alone after plastic deformation. This means that in Au only one self-interstitial configuration exists which, however, migrates in Stage III as postulated by the "two-interstitial model".

obtainable from mechanical measurements and microstructure observations may be deduced from measurements of the residual electrical resistivity and its recovery.

(*ii*) When pertaining to the same question, the results from electrical and mechanical measurements agree.

(*iii*) The observation that after low-temperature fatigue of Cu the recovery of the residual electrical resistivity does not start until the annealing temperature is raised to about 100 K is in serious conflict with the "one-interstitial model" but in full accord with the "two-interstitial model" of the radiation damage of fcc metals.

ACKNOWLEDGEMENT

The author would like to express his indebtedness to Professor Dr. Werner Frank for many discussions on self-organization processes and for his contributions to the sharpening of the key ideas of the present paper. The assistance of Miss Susanne Kammerer in the preparation of the text is gratefully acknowledged.

REFERENCES

1 A. Seeger, in: Proceedings 8th Intern. Conf. on the Strength of Metals and Alloys (P.O. Kettunen, T.K. Lepistö, and M.E. Lehtonen, eds.), Pergamon Press, Oxford 1988, p. 315.

2 H. Mughrabi, Mater. Sci. Engng. **33**, 207 (1978).

3 U. Holzwarth, Dr. rer. nat. thesis, Universität Stuttgart, Stuttgart 1992.

4 L. Hollang, M. Hommel, and A. Seeger, phys. stat. sol. (a) **160**, 329 (1997).

5 A.T. Winter, Phil. Mag. **30**, 719 (1974).

6 A.T. Winter, in: Fundamentals of Deformation and Fracture (Eshelby Memorial Symposium, Sheffield 1984; B.A. Bilby, K.J. Miller, and J.R. Willis, eds.), Cambridge University Press, Cambridge etc. 1985, p. 573.

7 A. Seeger and W. Frank, Solid State Phenomena **3&4**, 125 (1988).

8 W. Frank, Solid State Phenomena **3&4**, 315 (1988).

9 L.L. Lisiecki and J.R. Weertman, Acta metall. mater. **38**, 509 (1990).

10 A. Seeger, in: Dislocations and Mechanical Properties of Crystals (J.C. Fisher, W.G. Johnston, R. Thomson, and T. Vreeland, Jr., eds.), J. Wiley & Sons, New York 1957, p. 243.

11 A. Seeger and B. Šesták, phys. stat. sol. (b) **43**, 433 (1971).

12 F. Ackermann, H. Mughrabi, and A. Seeger, Acta metall. **31**, 1353 (1983).

13 C. Zener, Elasticity and Anelasticity in Metals, Univ. Chicago Press, Chicago 1948.

14 F.C. Frank and W.T. Read, Phys. Rev. 79, 722 (1950).

15 G. Lück and R. Sizmann, phys. stat. sol. **5**, 683 (1964); **6**, 263 (1964); **14**, 507 (1966).

16 A. Seeger, Radiation Effects **111**, 355 (1989).

17 A. Seeger, N.Y. Jin, F. Phillipp, and M. Zaiser, Ultramicroscopy **39**, 342 (1991).

18 Z.S. Basinski, A.S. Korbel, and S.J. Basinski, Acta metall. **28**, 191 (1980).

19 Z.S. Basinski and S.J. Basinski, Acta metall. **37**, 3255 (1989).

20 A. Seeger, Theorie der Gitterfehlstellen, in: Encyclopedia of Physics (S. Flügge, ed.), Volume VII, Part I, Springer, Berlin etc. 1955.

21 Z.S. Basinski and S.J. Basinski, Acta metall. **17**, 3275 (1989).

22 The Oxford English Dictionary, 2nd ed., Vol. XVII, p. 902, Clarendon Press, Oxford 1989.

23 W. Schilling, P. Ehrhart, and K. Sonnenberg, in: Fundamental Aspects of Radiation Damage in Metals (M.T. Robinson and F.W. Young, Jr., eds.), USERDA, Conf. 751006-P1, U.S. Department of Commerce, Springfield VA 1975, p. 470.

24 A. Seeger, in: Fundamental Aspects of Radiation Damage in Metals (M.T. Robinson and F.W. Young, Jr., eds.), USERDA, Conf. 751006-P1, U.S. Department of Commerce, Springfield VA 1975, p. 493.

25 A. Seeger, Phys. Letters **89A**, 241 (1982).

26 J. Briggmann, K. Dagge, W. Frank, A. Seeger, H. Stoll, and A.H. Verbruggen, phys. stat. sol. (a) **146**, 325 (1994).

27 T.H. Blewitt, R.R. Coltman, and J.K. Redman, in: Report on a Conference on Defects in Crystalline Solids, The Physical Society, London 1955, p. 369.

28 A. Seeger, in: Radiation Damage in Solids, Vol. I, IAEA, Vienna 1962, p. 101.